



**Final Design Report**  
**Group 1 – LUNARTICS**

David Bishop, Alex Brito, Kayla Garoust,  
Michael Gerber, Jeff Glynn, Austin Horrell

**EAS4700 Spring 2022**  
**Suborbital Lunar Transport**



# Table of Contents

<b>Acronyms List .....</b>	<b>6</b>
<b>Executive Summary .....</b>	<b>7</b>
Purpose .....	7
Team Organization.....	7
Schedule .....	7
Overview .....	7
Budget .....	9
<b>Conception of Operations .....</b>	<b>11</b>
Concept for Lunar Landing .....	11
Concept for Automated, Powered Descent .....	12
Concept for Lunar Transport and Return .....	13
Warm up at SCS .....	13
Transit to Forward Operating Base .....	14
Cooldown at Forward Operating Base .....	14
Return to SCS .....	15
Cooldown at SCS.....	15
Notes on the Concepts of Operations.....	15
<b>Structures.....</b>	<b>17</b>
Overview .....	17
Base Structure .....	17
Landing Gear.....	18
Structure Organization and Mounting.....	19
Fabrication and Manufacturing .....	20
Stress Analysis .....	21
Final Properties .....	24
<b>Mechanisms .....</b>	<b>24</b>
Payload Deployment Module (PDM) .....	24
Landing Gear.....	25
<b>Propulsion.....</b>	<b>27</b>
Overview .....	27
Selection Processes .....	27

Propellant Type.....	27
Main Engines .....	28
ACS Thrusters .....	30
Propellant Tanks .....	30
Trajectory .....	31
Valving .....	33
Cost.....	33
Valving Cost Information.....	33
Non-Valving Cost Information.....	34
Risk Assessment.....	35
<b>Guidance and Navigation.....</b>	<b>36</b>
Overview .....	36
Typical Flight Operation .....	36
Descent and Landing.....	37
Vehicle Health.....	38
Risk Assessment.....	39
<b>Communications .....</b>	<b>41</b>
Overview .....	41
Risk Assessment.....	41
<b>Environmental.....</b>	<b>43</b>
Thermal .....	43
Thermal Environments and Requirements .....	43
Thermal Control .....	44
Thermal Concerns & Risk Management .....	46
Vibroacoustic .....	46
Vibroacoustic Environments .....	46
Vibroacoustic Control.....	47
Vibroacoustic Concerns & Risk Management .....	49
<b>Electrical .....</b>	<b>50</b>
Overview .....	50
Inventory .....	50
Power Requirements .....	51

Cable Routing.....	52
Risk Assessment.....	53
<b>Testing.....</b>	<b>55</b>
<b>References.....</b>	<b>58</b>
Structures.....	58
Mechanisms.....	59
Propulsion.....	60
Guidance and Navigation .....	61
Communications.....	62
Environmental .....	63
Electrical.....	64
<b>Testing.....</b>	<b>65</b>
<b>Appendices.....</b>	<b>66</b>
Appendix A: Open Items Status Report.....	66
Appendix B: Trade Studies .....	67
Structures .....	67
Mechanisms .....	68
Propulsion.....	70
Guidance and Navigation .....	71
Communications.....	73
Environmental .....	75
Electrical.....	77
Appendix C: Calculations .....	79
Structures .....	79
Propulsion.....	82
Guidance and Navigation .....	84
Communications.....	85
Environmental .....	86
Appendix D: Requirements Matrices.....	87
Appendix E: Engineering Change Notices.....	89
Structures .....	89
Mechanisms .....	90

Guidance and Navigation .....	91
Communications.....	93
Appendix F: SLT Size Verification .....	95
Appendix G: Center of Mass and Mass Properties .....	97

## **Acronyms List**

ACS – Attitude Control Systems	NTO – Nitrogen Tetroxide
CDR – Critical Design Review	PDM – Payload Deployment Module
CPL – Co-manifested Payload	PDR – Preliminary Design Review
ECN – Engineering Change Notice	PMAD – Power Management and Distribution
ECVT – Electrical Capacitance Volume Tomography	PVT – Pressure-Volume-Temperature
FEA – Finite Element Analysis	RHC – Right Hand Circular
FoS – Factor of Safety	ROSA – Roll Out Solar Array
GHe – Gaseous Helium	SCS – Shackleton Crater Station
GNC – Guidance and Control	SDR – Software Defined Radio
HDL – Hazard Detection Lidar	SLT – Suborbital Lunar Transport
IMU – Inertial Measurement Unit	SPLICE – Safe and Precision Landing Integrated Capabilities Evolution
ME – Main Engine	TRL – Technology Readiness Level
MMH – Monomethyl Hydrazine	TRN – Terrain Relative Navigation
MON – Mixed Oxides of Nitrogen	TWR – Thrust-to-Weight Ratio
NDL – Navigation Doppler Lidar	
NRHO – Near-Rectilinear Halo Orbit	

# Executive Summary

## Purpose

In order to support NASA astronauts operating around the Shackleton Crater Station (SCS) at the lunar south pole, there is a need to design a Suborbital Lunar Transport (SLT) with the ability to deliver payloads to astronauts too far for ground-based transport to be feasible. As outlined in document DSG-RQMT-001, the SLT is intended to be a semi-autonomous unmanned craft that is both reusable and multifunctional, and capable of hauling 200 kilograms of payload to and from a forward base of operation up to 300 kilometers from SCS. The SLT must also be capable of deorbiting and landing from a near-rectilinear halo orbit (NRHO) after insertion from the Space Launch System (SLS) as a co-manifested payload (CPL). This report presents a preliminary design of the SLT with a proposed launch date of November 2030.

## Team Organization

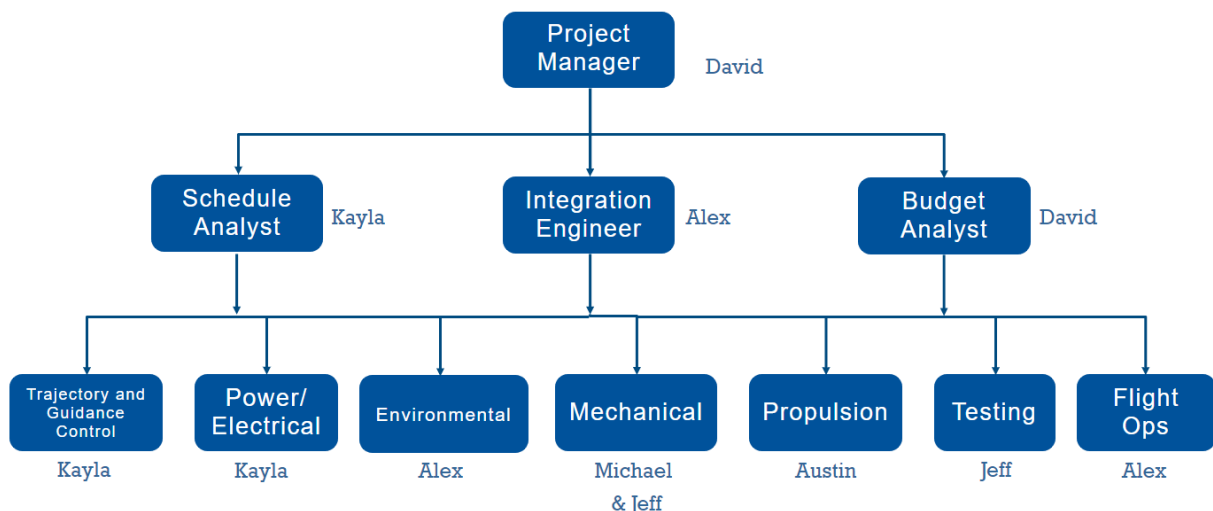


Figure 1. Graphical representation of the team organization.

## Schedule Overview

The current schedule allows for a three-year “buffer” period between the end of testing and the given launch date to account for any failures or mishaps during testing or manufacturing. The launch date is set for November 2030, but this is subject to change. Manufacturing and testing are expected to begin as soon as the final design is approved (May 2022). Once the final design has been approved, the purchasing of parts from suppliers can also begin. It is expected for launch site processing to take around 5 years, however the SLT will not need to be shipped out to the launch

site until 6 months prior to launch. See the figures below for a more detailed breakdown of events between now and launch. The testing schedule is reviewed in further detail in the testing section.



Figure 2: Breakdown of schedule from Final Report through Launch Site Processing.



Figure 3: Breakdown of schedule through Launch Site Processing.

## Budget

Total Budget	USD
First Unit Total Allotted	400,000,000
Design Actual Cost	19302161.08
Manufacturing Actual Cost	50,000,000
Testing Actual Cost	24,400,000
First Unit Actual Cost	93702161.08
5 year Operational Cost	1,500,000,000

*Figure 4. Summary of Budget.*

The overall budget summary is provided in the figure above. \$400 million is the total budget allotted which includes all design, labor, and manufacturing costs. The actual cost to produce the first unit is predicted to be just under a quarter of the allotted budget at \$93.7 million. To operate the spacecraft for five years following the initial deployment, \$1.5 billion is allotted. The next table shown displays a more detailed cost breakdown of each system. Please refer to the testing section for a more detailed breakdown of the testing budget.

Much of the itemized breakdown consists of costs associated with purchasing production units from various suppliers. Many of these highly specialized parts, systems, and sensors are made in low production numbers or even made to order, hence the relatively high costs, although this is typical of most aerospace applications. An estimated labor cost of ten million dollars is made up of one hundred salaries worth, which is equivalent to approximately five years of development for twenty engineers.

	Quantity	Cost Per	Total Cost
<b>Guidance, Control, Communication</b>			
Star Tracker	3	50,000	150000
Sun Sensor	8	12,000	96000
Inertial Measurement Unit	2	10,000	20000
Reaction Wheels	4	15,000	60000
Flight Computer	2	200,000	400000
SDR	2	30,000	60000
X-Band Antenna	2	4,500	9000
S-Band Antenna	2	4,500	9000
X-Band Amplifier	2	2,200	4400
S-Band Amplifier	2	5,000	10000
Cameras	7	10,000	70000
NDL	1	35,000	35000
HDL	1	45,000	45000
Altimeter	2	8,000	16000
Descent Computer	1	175,000	175000
<b>Electronics</b>			
Solar Panel	1	50,000	50000
Li-Ion Battery	10	50,000	500000
PMAD	2	50,000	100000
Wiring	5000	10	50000
<b>Environmental</b>			
Multi-Layer Insulation (m^2)	20	512	10240
Shockwave Dampers	15	117	1755
Melamine Foam	17	30	510
Radiator	1	580	580
Heat Pipes	1	300	300
Thermal Fluid	1	590	590
<b>Propulsion</b>			
Main Engines	4	1,000,000	4000000
Thrusters	8	250,000	2000000
Pressure Regulator	3	4,000	12000
Pressure Transducer	11	5,000	55000
Solenoid Valve	18	7,500	135000
Inlet Isolation Valve	16	7,500	120000
Latch Valve	8	4,000	32000
Fill/Drain Valves	5	1,500	7500
MNH	947.8	147	138890.612
MON-3	1990.3	152	302386.279
Helium	0.0841	33	2.792961
Propellant Tank	2	75,000	150000
Pressurant COPV	1	50,000	50000
Piping	1	5,000	5000
<b>Structures &amp; Mechanisms</b>			
Aluminum 7075-T6	342	6	2052
PDM Battery	1	270	270
PDM Locking Motor	1	684.4	684.4
PDM Deployment Motor	4	100,000	400000
Shock Absorber	4	2,000	8000
<b>Labor and Misc</b>			
Fasteners	1000	5	5000
Fittings	1000	5	5000
Labor	100	100,000	10000000

Figure 5. Detailed system by system budget breakdown.

## Conception of Operations

The Lunartics Suborbital Lunar Transport (SLT) is a semi-autonomous craft designed to support astronauts at Shackleton Crater Station (SCS). It does this by transporting up to 200 kg of supplies from SCS to a forward operation base up to 300 km away, landing itself in a safe spot.

The SLT will begin its mission as a co-manifested payload with the ORION space capsule on NASA's SLS vehicle. The SLS will inject the SLT into a near-rectilinear halo orbit around the moon. From there, it will land on the lunar surface near SCS and begin its standard mission operations.

The standard mission operation would be waiting for a support signal from an operational site, transporting supplies to the site, allowing for waste to be loaded onto the SLT, and then returning to SCS.

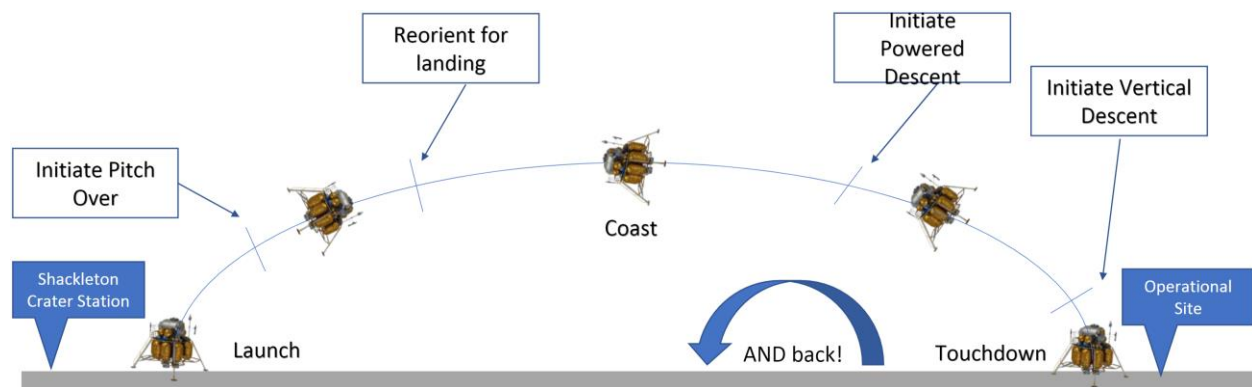


Figure 6. Depiction of SLT trajectory.

## Concept for Lunar Landing

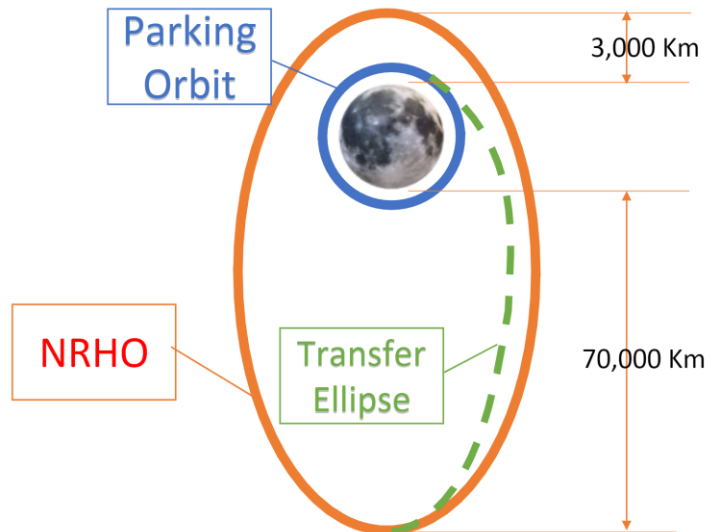


Figure 7. Diagram showing initial orbit transfer.

1. SLT is taken to a near rectilinear halo orbit around the moon using the SLS.

2. SLT will run a diagnostic to ensure propulsion, guidance, and communication systems are functioning nominally.
3. At apolune of orbit, SLT will begin a retrograde burn to enter a transfer orbit, leading to a 100 km parking orbit.
4. When approaching the Lunar north pole, SLT will begin a retrograde burn to deorbit. This transfer orbit will have an apolune of 100km over the lunar north pole and a perilune of 17.5km.

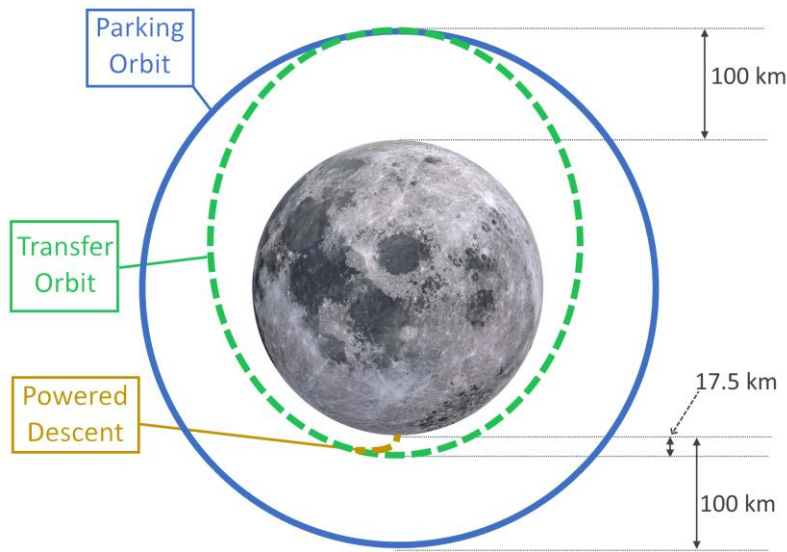


Figure 8. Diagram showing transfer from orbit to descent.

5. Astronauts at Shackleton Crater Station (SCS) will clear landing space for SLT and ensure area is clear of objects and personnel.
6. The SLT will remain in transfer orbit until receiving confirmation from SCS to begin landing sequence. Simultaneously, the SLT will run a diagnostic to ensure any systems required for landing are nominal.
7. When approaching the periapsis of the transfer ellipse, powered descent (PD) is performed.
8. Once SLT is landed, main engine is powered down and SLT enters standby until cooled.

### Concept for Automated, Powered Descent

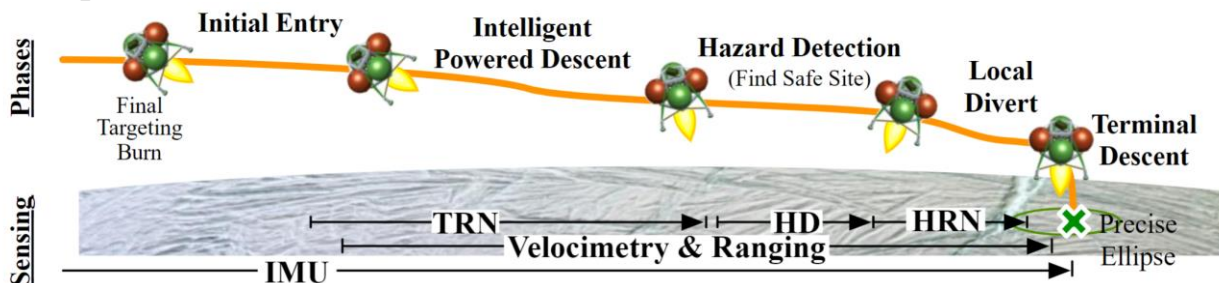


Figure 9. Diagram of SPLICE technology and the phases of different components.

1. IMU operations switch over to IMU dedicated to descent and landing
2. Cameras take pictures of moon's surface and compare to stored images for TRN
3. At 6.4 km from the surface, the NDL and altimeter activate to detect speed and range
4. Lander rotates to vertical upright orientation
5. At 500 m from the surface, HDL activates and scans for hazards
6. Hopper lands within 10 m ellipse

## Concept for Lunar Transport and Return

### Warm up at SCS

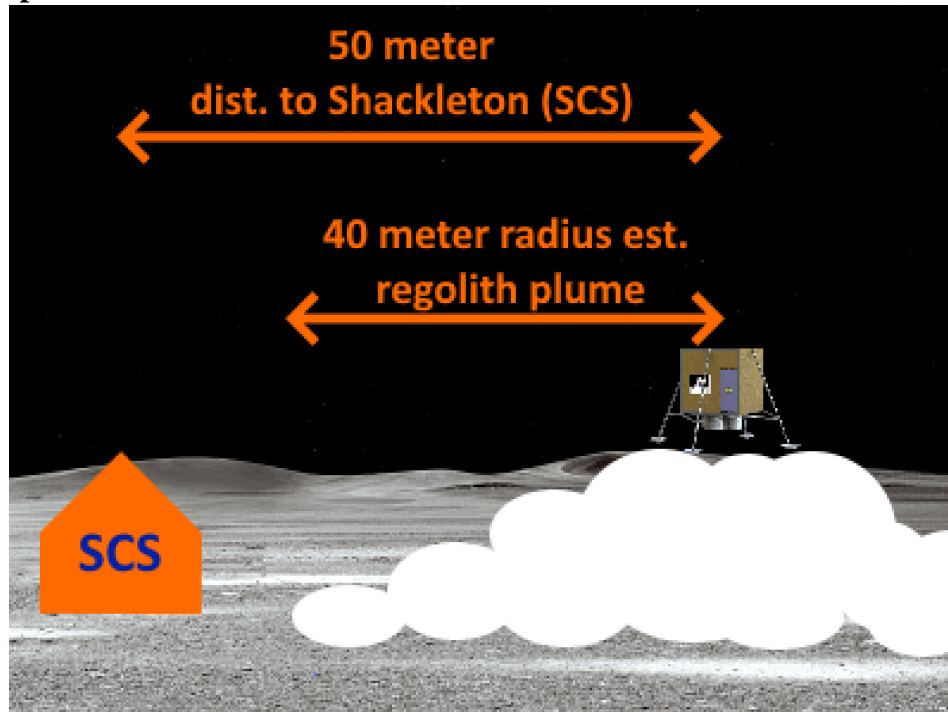


Figure 10. Illustration of regolith plume from SLT.

1. Signal is sent by astronauts at forward operating base requesting supplies and giving location data.
2. Astronauts at SCS load the specified supplies. Payload mass data is uploaded to SLT.
3. Flight computers run calculations to develop a flight path and fuel requirements. Flight path and fuel requirements are compared between flight computers for redundancy.
4. SLT is charged and fueled by astronauts at SCS to specification.
5. Fuel and power lines removed by astronauts at SCS.
6. Astronauts clear out a 50m area around SLT of equipment and personnel.
7. SLT begins diagnostic to make sure all systems are functioning nominally.

## Transit to Forward Operating Base

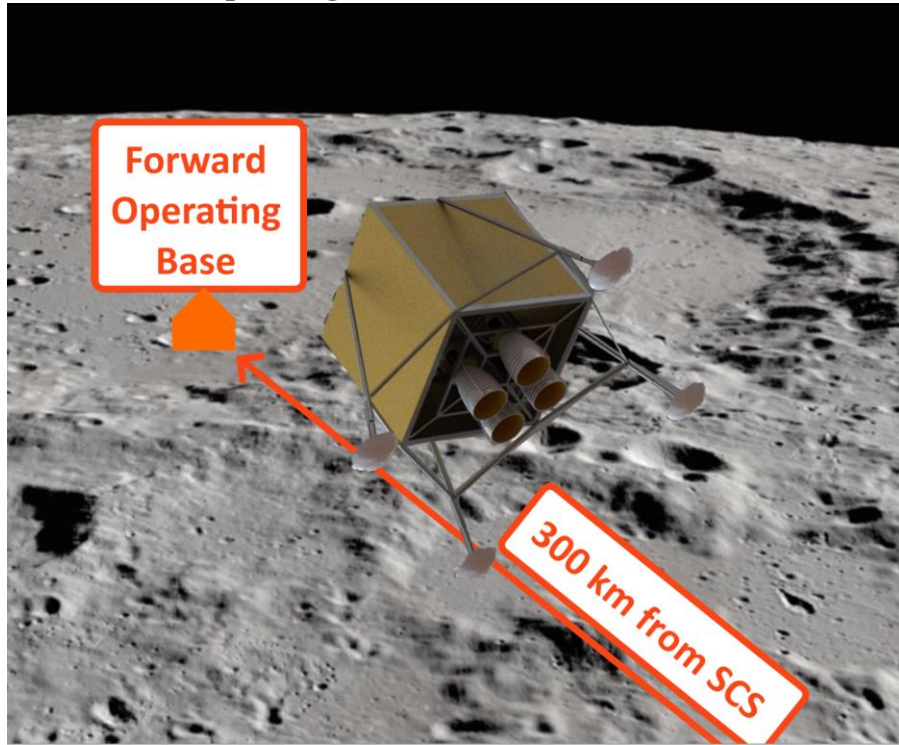


Figure 11. Depiction of the moon's surface showing the range for the SLT.

1. Low thrust using 2 engines at low altitudes.
2. Increase thrust and activate secondary engines at higher altitudes after pitch over to reduce regolith spread around SCS.
3. Initiate pitch over using attitude control thrusters.
4. Disengage main engine to enter coast phase.
5. Initiate attitude control thrusters to orient SLT for landing.
6. Initiate powered descent around landing site.

## Coldown at Forward Operating Base

1. Power down main engine and allow for system to cool.
2. SLT enters standby mode where thermal requirements are kept, and communications systems are kept powered.
3. Payload is removed from SLT and replaced per astronaut's needs. Astronauts communicate new mass data to SLT
4. SLT receives return signal from SCS. Powers on flight computers to calculate return trip from current landing zone. Return trip data from each computer is compared for redundancy.
5. Astronauts clear out a 50m area around SLT of equipment and personnel.
6. SLT begins diagnostic to make sure all systems are functioning nominally.

## Return to SCS

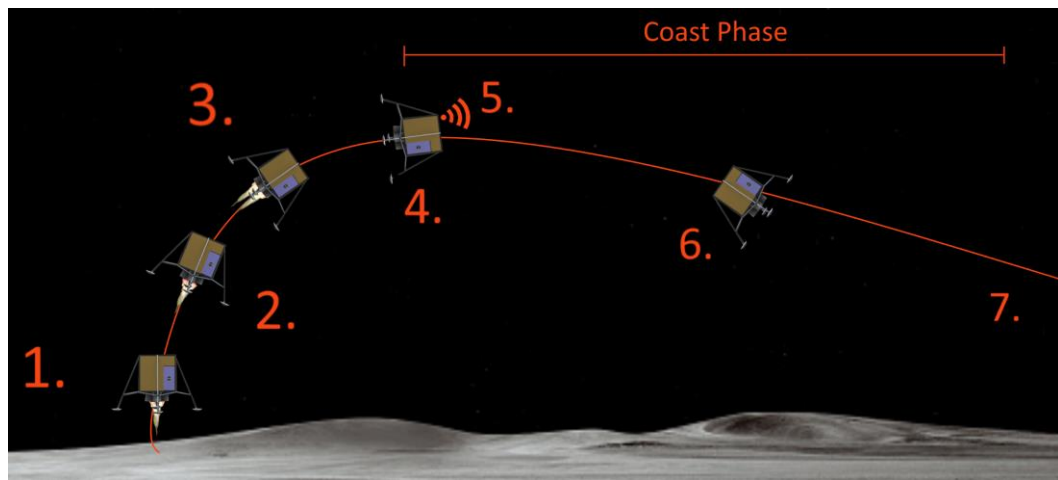


Figure 12. Trajectory of the SLT on the return trip.

1. Low thrust using 2 engines at low altitudes.
2. Initiate pitch over
3. Increase thrust and activate secondary engines at higher altitudes after pitch over to reduce regolith spread around SCS.
4. Disengage main engine to enter coast phase
5. Notify SCS ground crew to clear out the designated landing site near SCS.
6. Initiate attitude control thrusters to orient SLT for landing
7. Initiate powered descent around designated landing site near SCS.

## Coldown at SCS

1. Power down main engine and allow for system to cool.
2. SLT enters standby mode where thermal requirements are kept, and communications systems are kept powered.
3. SLT is attached to power and fuel lines at SCS.
4. Power is drawn from SCS and onboard batteries are disabled.
5. Leftover fuel is pumped back to SCS

## Notes on the Concepts of Operations

The required  $\Delta V$  for lunar landing was estimated to be 2608.6 m/s. This was comparable to the required  $\Delta V$  for a round trip mission of around 2800 m/s. In fuel calculations, both were estimated to be 5% greater to allow for extra buffer for landing hazard avoidance. A table of  $\Delta V$  requirements can be found below.

Action	$\Delta V$ Required [m/s]
NRHO to 100km circular parking orbit	730
Deorbit Burn to establish a 100km x 17.5km transfer ellipse	18.6
Powered Descent	~1860
300 km Round Trip Mission	~2800 + 5% extra for landing hazard avoidance

Figure 13. Impulses required at each phase.

Another note of importance was the selection of a 50m “safety area” around the SLT to avoid regolith. This was designed as a mission requirement for the SLT project was to keep astronauts safe from regolith ejected by the SLT’s thrusters. First, research was done on exhaust plumes of space craft on the moon. A historical study by the science definition team on NASA’s Artemis project found a quadratic relation between the dry mass of the craft and the exhaust plume radius with a coefficient of determination of 0.91. This implied that using this estimate would provide a close value, though it would have to be refined during testing. To allow for extra safety of astronauts, the exhaust plume estimate of 40m was multiplied by an extra 25% to determine a safe area for astronauts.

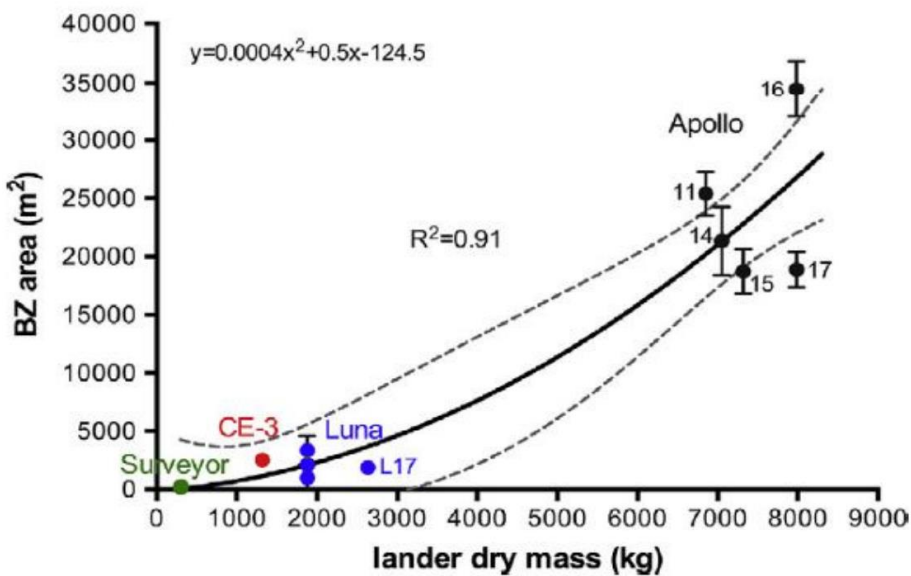


Figure 14. Graph of BZ area against dry mass.

# **Structures**

## **Overview**

The design of the SLT structure was primarily driven by the requirement that the SLT could not exceed 2000 kg at launch excluding the payload (ASD-SLT-09). Outside of this, the two main derived requirements for the sizing of the SLT from the given requirements (ASD-SLT-01 and ASD-SLT-010 to ASD-SLT-016) were that the SLT must fit inside the 8.4 m capsule on the SLS and that the SLT must be capable of accommodating a 200kg payload of volume 1.2m x 0.5m x 0.5m while still maintaining a proper operational center of gravity. Overall, the structure needed to have a low mass but a high strength to be capable of replicating multiple missions. Due to this, Aluminum 7075-T6 was selected as the primary material for the base structure as well as for the landing gear and footpads. A trade study for this decision is documented in Appendix B. Although Aluminum 7075-T6 didn't win the trade study it was selected over carbon fiber mainly because carbon fiber has low machinability and a limited history of acting as the primary structure for a spacecraft experiencing repeated loads due to landing and takeoff. Aluminum 7075-T6 also has a high strength compared to similar aluminum alloys and it was selected because it has better corrosion resistance than Aluminum 7178-T6. The SLT was also designed around a minimum factor of safety (FoS) of 2.0 because in spacecraft design this is commonly considered an acceptable FoS for ground handling equipment. The base structure of the SLT is a cubic aluminum truss that is welded together. The landing gear is connected to the base structure using Ti-6Al-4V connections instead of welding for increased strength, corrosion resistance, and for easier repairability if one or multiple landing legs get damaged.

## **Base Structure**

The base structure for the SLT is a cubic truss made from Aluminum 7075-T6. It is composed of thin-walled hollow rectangular truss members welded together at the ends. There are several interior struts which were designed to support the various equipment needed by other subsystems such as engines, propellant tanks, and electrical equipment. The rectangular profile struts were initially circular but were adjusted in order to allow for easier mounting of objects with rectangular profiles such as panels, star trackers, and patch antennas. The base structure can be seen in Fig. 15 below.

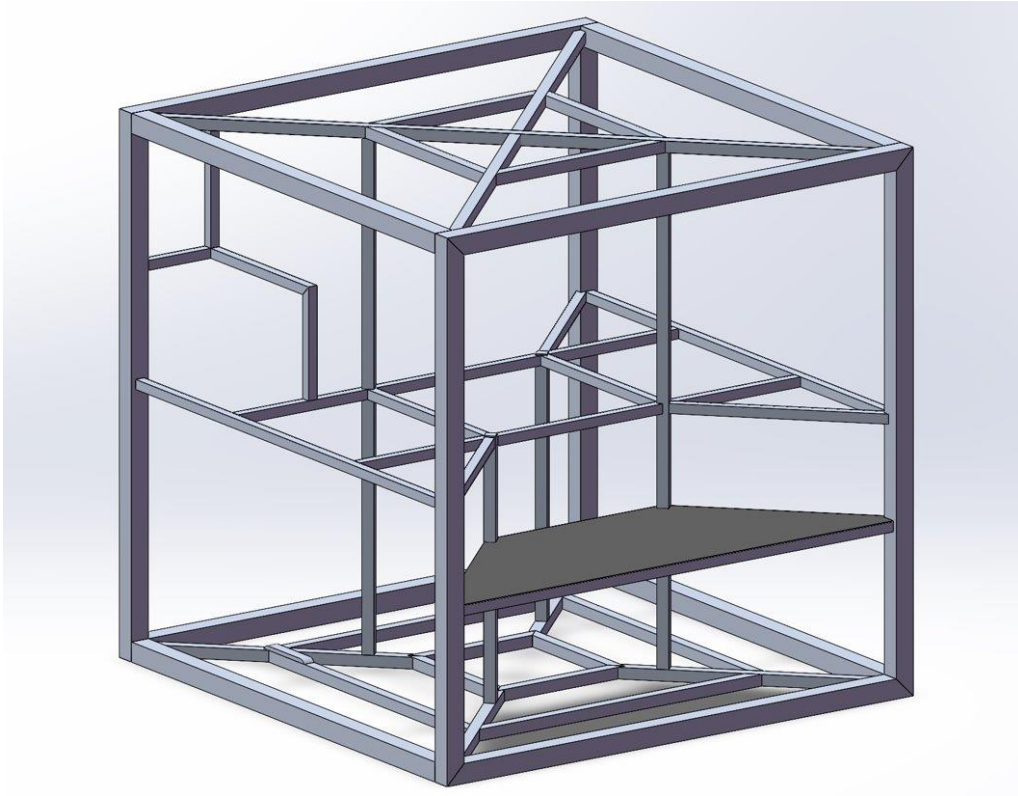


Figure 15. Base structure of the SLT.

## Landing Gear

The landing gear for the SLT was designed with four legs equally spaced around the cubic truss for stability. A cantilever landing configuration was chosen instead of an inverted tripod configuration in order to save mass by having shorter secondary struts. The landing gear struts are made of thin-walled hollow cylindrical tubes which are welded to titanium connectors on each end. Each of the four landing legs consists of one primary strut and two secondary struts. Each primary strut is divided into two sections: a thicker circular strut which houses the shock absorber (more details in the Mechanisms section) and a thinner circular strut which slides into the thicker strut and absorbs the shock during landing. The titanium connector on the larger end of the primary strut is attached to a rotational hinge joint that is welded to the top of the base structure while the titanium connector on the smaller end is attached to a rotational hinge welded on the footpad which allows for the SLT to land on varying slopes. For the secondary struts, one end is connected to an aluminum extrusion at the bottom of the base structure and the other end is welded to the thicker section of the primary strut. An image of the landing gear on one side of the SLT is shown in Fig. 16 below.

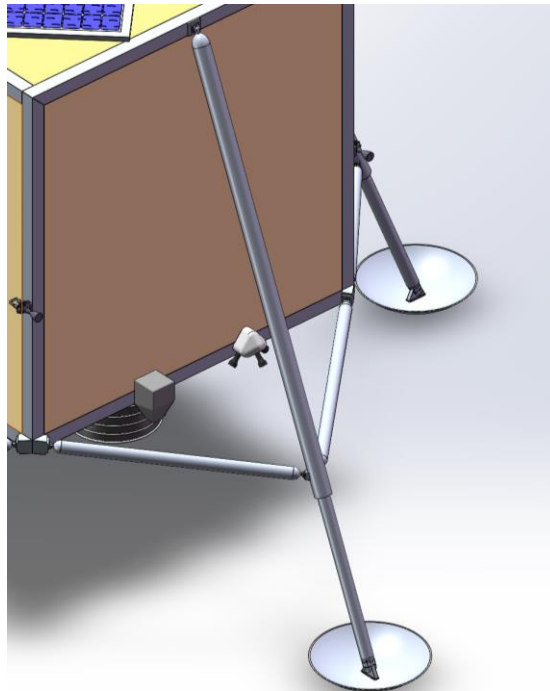


Figure 16. Landing gear on one side of the SLT.

## Structure Organization and Mounting

From Fig. 17 below, the mounting and organization of various components on the SLT can be seen.

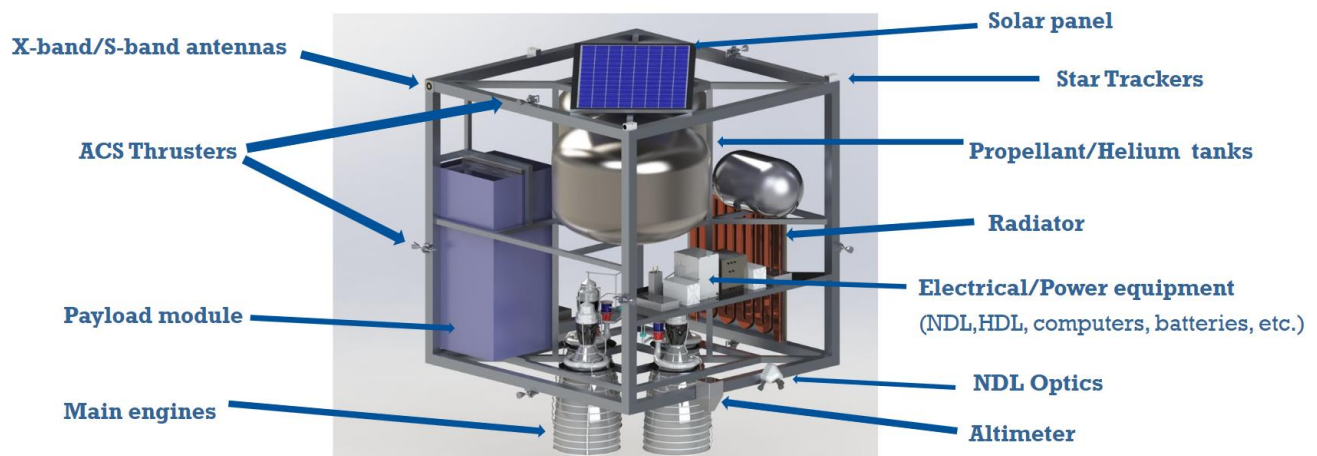


Figure 17. Isometric view of the SLT organization (with insulation and wiring hidden).

Starting at the top of the structure a solar panel is mounted on top of one of the insulation panels (hidden from figure). Moving down the structure, the propellant tanks sit on the top shelf

of the truss and are positioned on opposite corners of the SLT while remaining within the frame of the cubic truss. The main bipropellant tanks are welded on their top and bottom surfaces to the struts going across the truss, while the helium tank is rotated so that its axis is parallel to the top plane of the cube and then welded to the top shelf of the truss. The elbow joint hanging down from the top of the truss serves as the mount for the payload module. The payload deployment module slide-out rail is welded to the bottom surface of this strut. A radiator is positioned on one side of the truss and there are five insulation panels surrounding the SLT to allow for thermal control (hidden from figure). The bottom shelf of the truss houses various electrical/power equipment such as the NDL, HDL, flight computers, and batteries. Four engines are welded equally distanced apart along the central cross-bracing at the bottom of the truss. There are two sets of four ACS thrusters on opposite sides of the SLT allowing for movement and rotation in all three X-Y-Z directions. There are also other various instruments mounted along the exterior of the frame, such as star trackers, patch antennas, and laser altimeters.



*Figure 18. Front, back, and top views of the SLT with insulation and wiring hidden.*

## Fabrication and Manufacturing

Most of the SLT's components were chosen to be welded together. This was because welding is efficient for long-term use similar to the expectations of this mission as welding seals the structure and is relatively stronger than bolted joints. Welded joints were also chosen because they take up less mass than bolted joints. A big downside to this however is that welding aluminum and welding specific aluminum alloys like Aluminum 7075-T6 is difficult due to the formation of cracks. To account for this, we have made sure to include adequate time and money in the schedule and budget to ensure that all the aluminum members are welded together correctly. One possible solution we hope to utilize is infusing titanium-carbide nanoparticles into wire that serves as the weldment filling material. It has been found that this wire can be used in arc welding to create welded joints that do not have any cracks.

There will also be some parts of the SLT that are secured by fasteners such as the landing struts and footpads. The landing gear and its joints are expected to experience the most fatigue and possible failure due to repeated missions and landings. Due to this, the landing gear was chosen to be secured using titanium fasteners for added strength and also so that landing gear can be easily repaired without needing to alter other sections of the structure. These connections were also

chosen to be machined to be the same time so that astronauts will need less tools to repair the connections. The titanium fasteners will be difficult to machine, but there is adequate time and money in place in the schedule and budget to account for the resources needed to get the parts from manufacturers.

## Stress Analysis

A stress analysis was conducted on the two most predominantly loaded portions of the structure. This would be the landing legs during landing and the engine mounts under maximum thrust operation. To begin the analysis, a preliminary fatigue analysis was conducted. The total number of missions was determined based on the life expectancy and mission frequency of the craft. Reducing the yield strength of the material through fatigue was deemed to have a negligible effect based on the S-N curve for the material chosen for the main structure of the vehicle.

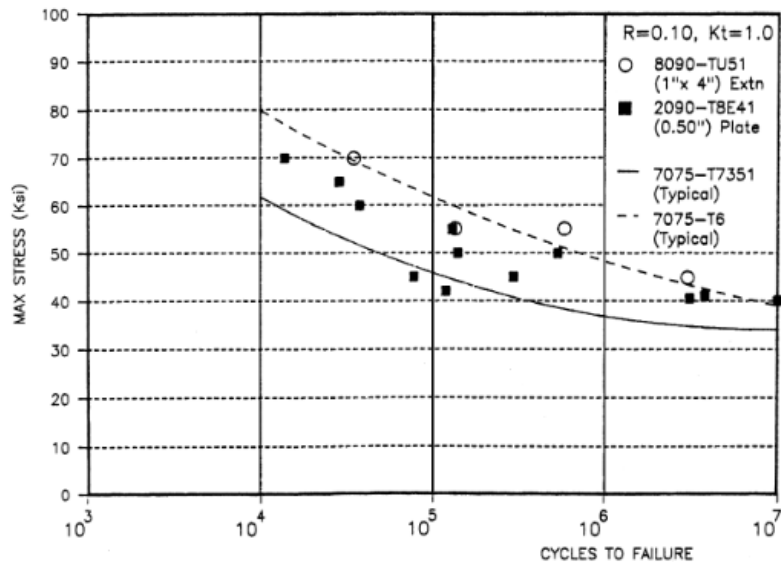


Figure 19. S-N Curve for several metals.

The second step taken in the analysis was to determine if the extreme temperature variations encountered in the lunar environment play a role in affecting the yield strength of the material. The highest temperature seen in the moon is roughly 390 K, and the yield strength can be seen to reduce approximately 10%, which will be used in the following finite element analysis models. The lowest temperature expected to be encountered is about 40 K. The figures below show the strength of 7075 does not decrease significantly due to cold temperatures.

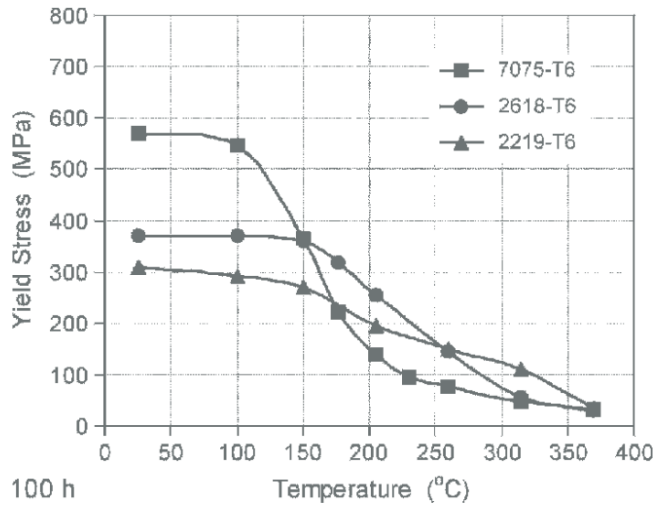


Figure 20. Stress vs temperature curves for several materials.

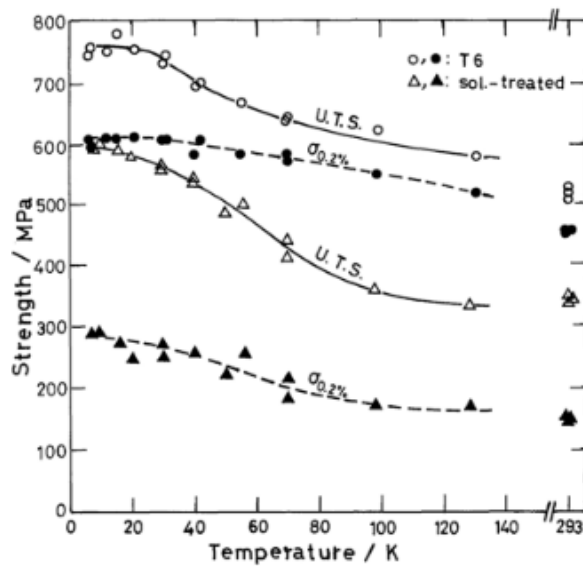


Fig. 2 Temperature dependence of 0.2% proof stress and ultimate tensile strength in T6 and solution-treated specimens.

Figure 21. Stress vs temperature curves for 7075.

The next step was to conduct finite element analysis using SolidWorks simulation tool on the landing legs and engine mounts. An upwards load on the feet of twice the static weight was used to simulate not landing on all four legs simultaneously. The simulation revealed that the lowest factor of safety is approximately three. This allows some breathing room for unexpected harsh landings. This simulation also revealed that internal bracing on the main structure in the payload bay of the SLS may be needed if the peak acceleration leaving Earth is to exceed 5 G's.

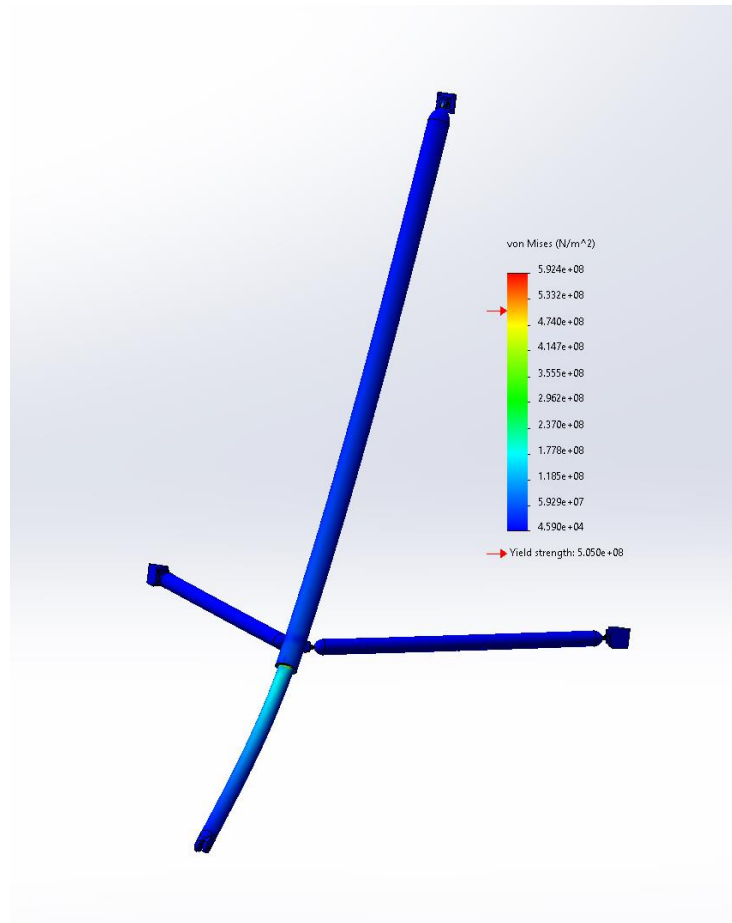


Figure 22. Landing leg FEA.

Like the landing leg simulation, a static loading simulation was conducted on the main structure where the four main engines mount. The load applied was equivalent to all four engines operating at a maximum thrust condition.

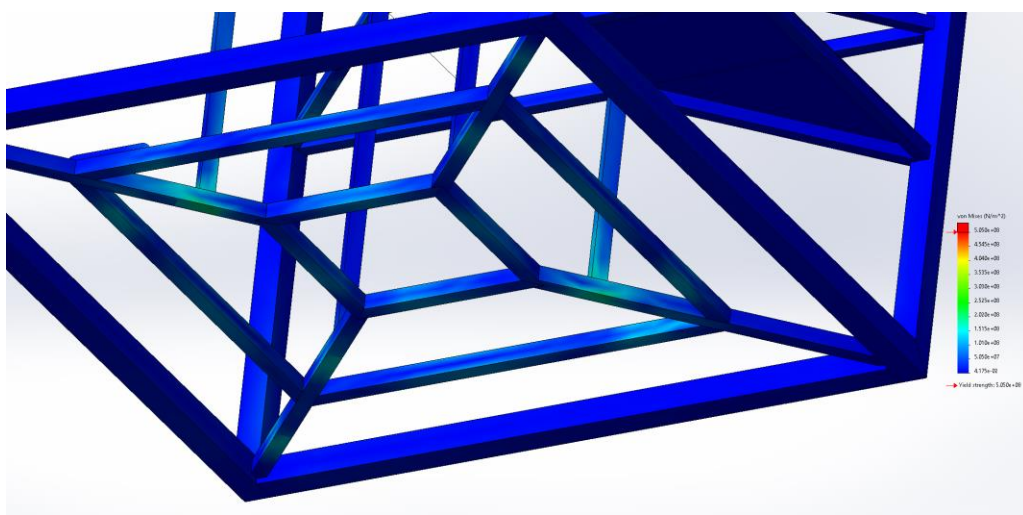


Figure 23. Engine mount FEA.

The lowest factor of safety seen in the engine mounting section of the main structure is approximately 2, which matches the advised factor of safety for structural components. For all scenarios, the stresses remain under the yield strength of the material, meaning ultimate stress is not reached.

## Final Properties

In Appendix F, Fig. 82 shows the size of the SLT and Fig. 83 shows that the SLT comfortably fits in the 8.4 m diameter SLS payload capsule with about 1.02 m from the outer footpad circle on each side to the inner wall of the payload capsule. In Appendix G, the total mass of the vehicle is documented, and other mass properties are listed. Fig. 84 shows the center of mass of the SLT with the payload removed. From these views it is seen that the center of mass is centrally located and is properly aligned with the ACS thrusters on the vertical struts. Fig 85 shows the center of mass with the payload included. From these views it is seen that with the payload included the center of mass is still centrally located and only slightly shifts toward the payload module by a few inches.

## Mechanisms

### Payload Deployment Module (PDM)

The payload deployment module or PDM for short was designed as drawer that slides out linearly. This decision was made based on simplicity and to reduce possible errors.

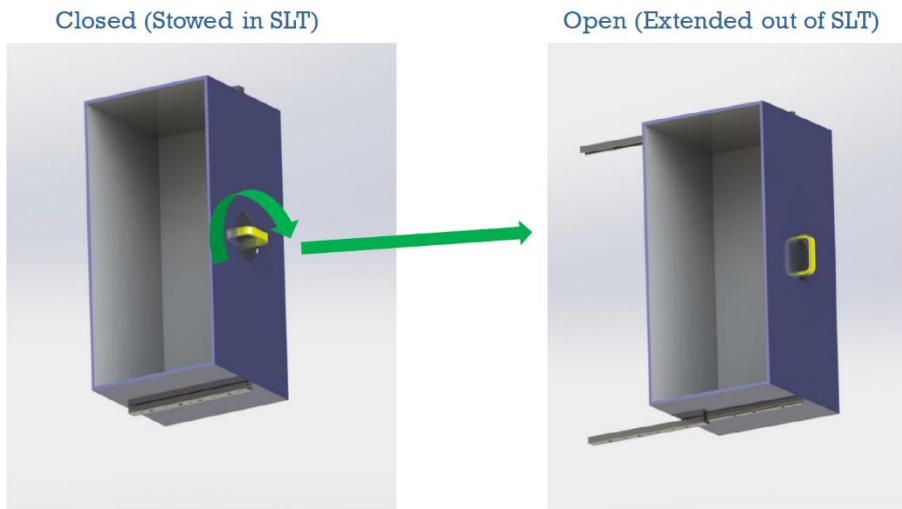


*Figure 24. Payload Deployment Module*

The PDM was designed to fit all specified payloads for the mission. It has dimensions of 1.3m by 0.6m by 0.6m to give a little extra room for any payload. The PDM also contains straps that will secure the payload into the drawer. The PDM can be deployed both manually and

remotely. To deploy the PDM manually, an astronaut can grab the ergonomic handle, twist 90 degrees to the unlocked position and then the drawer can be easily pulled out and the payload accessed. To deploy the PDM remotely, a signal can be sent to the on-board X-band radio. The PDM contains its own battery to power the two remote deployment motors. This extra battery adds security to the PDM. Since the main objective of the mission is to deploy and recover payload, the extra battery acts as a failsafe in case anything goes wrong with the main power source of the SLT, the mission would not be jeopardized. When the signal is given for deployment through X-band radio, The battery will power one motor that works to keep the PDM locked and one motor that works to slide out the payload drawer.

Trade studies were conducted for the battery, the locking motor, and the deployment motor. Further research and testing would allow for the chance to come up with solutions for some of the areas of concern with the system. These concerns include, payloads may become loose if an astronaut does not properly secure it with straps, and if the locking mechanism were to be stuck or keep the payload drawer from deploying, astronauts may have trouble unlocking the PDM and fixing the issue.

## Landing Gear

For the landing gear, the first thing that needed to be sorted out was whether the SLT should have deployable or static landing legs. The benefits of having legs that can be deployed are that they reduce the SLTs size when storing it in the SLS payload envelope. This would reduce the launch price of the SLT since it can be used as a co-manifested payload. The main issue with developing such a deployable landing leg system is its complexity. With added hardware and software, a deployable landing leg system could bring more failure points. To confirm this, a trade study was conducted.



*Figure 25. Landing legs.*

The next design decision regarding the landing legs was the type of shock absorbers to be used. Currently, the space industry has mostly used non-reusable crush honey-comb shock

absorbers, sometimes in series with hydraulics. These systems are not reusable, for our purpose, a reusable shock absorber system is imperative. We began by exploring our options from previous or developing technologies. These included, hydraulic damping, metal bellows shock absorbers, and electromagnetic shock absorbers. To further investigate their qualities, a trade study was conducted between them. The trade study was conclusive that the developing technology of the metal bellows shock absorbers was a good option for a reusable shock absorber. Because they are hermetically sealed the leaking risk of using a hydraulic system is greatly reduced and does not need an extensive thermal management system due to the lack of any fluid in the system. Hollow bellows shock absorbers work by utilizing a hermetically sealed chamber of air as well as a piston that utilizes metal bellows as sort of a spring and a small orifice of air that slowly allows air to flow past the piston. This design is much simpler than the electromagnetic shock absorbing system.

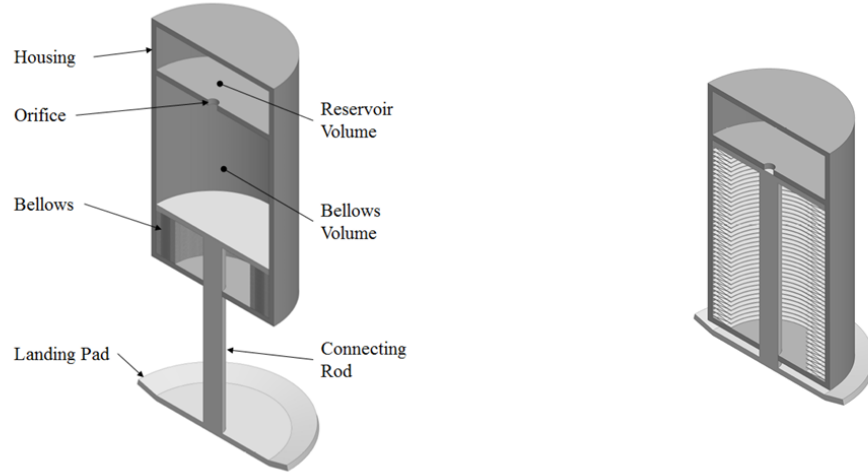


*Figure 26. Metal Bellows Shock Absorber*

Due to the landing legs utilizing the developing technology of metal bellows shock absorbers, further research and testing needs to be allocated towards making sure the system is reliable and functions properly.

# Propulsion

## Overview

Development of the propulsion system for the SLT consisted of a traditional trade-study-driven component selection, starting with the most overarching system-wide decisions and narrowing down eventually to individual component selection. The propulsion system is comprised of thrusters for both ascent/descent and attitude control.

As detailed below, the SLT uses a liquid hypergolic bipropellant propulsion system for its main engines (MEs) and its attitude control system (ACS), relying on monomethyl hydrazine (MMH) as fuel with nitrogen tetroxide (NTO) as oxidizer. These are pressure-fed using gaseous helium (GHe) as a pressurant. Four S3K engines manufactured by DASA provide ample thrust at exceptionally high specific impulse ( $I_{sp}$ ), while eight DST-12 ACS thrusters manufactured by Moog provide pitch/roll/yaw capability paired with the reaction wheels discussed in the Guidance and Navigation section.

## Selection Processes

The selection process for each aspect of the SLT propulsion system, including the list of objectives considered in subsystem trade studies, is outlined in the following subsections.

### Propellant Type

Chemical propulsion, as opposed to non-chemical (e.g. electric) propulsion, was selected for the SLT due to its payload (ASD-SLT-015) and range (ASD-SLT-020) capability requirements of 200 kg and 300 km, respectively; existing non-chemical propulsion methods do not generate the thrust levels indirectly required by DSG-RQMT-001. Additionally, solid chemical propellants were not considered: although some newer solid chemical propellant technologies allow for multiple restarts, few are flight-proven and none currently exist in the required thrust range.

A trade study considered four different propellants: hydrazine ( $N_2H_4$ ) with a catalyst bed; MMH and NTO; and two cryogenic bipropellant combinations, either liquid hydrogen ( $LH_2$ ) or liquid methane ( $LCH_4$ ) with liquid oxygen (LOX). Though full decision matrices are provided in Appendix B, table summarizing the objective considerations in propellant selection is given in the table on the following page:

Objective	Characteristic Measured
Bulk density, $\rho_b$	Packaging/containment efficiency
Characteristic velocity, $c^*$	Combustion efficiency
Thermal Sensitivity	Thermal regulation difficulty/complexity
Corrosivity	Potential to damage pipes, valves, etc.
Heritage	Historical reliability

MMH and NTO was chosen as the best propellant of the four, scoring a total of 209.8 points. For the sake of simplicity, ACS thrusters shared propellant with MEs; no obvious benefits would arise from using a separate propellant for attitude control.

Since MMH and NTO are both extremely toxic to humans and can be corrosive depending on the material and exposure time, care was taken in developing appropriate propellant handling procedures. One design decision made primarily due to the corrosivity requirements of the propellant was propellant line material choice: non-corrosive aluminum was used, rather than a ferrous metal, due to unwanted chemical interactions between hydrazine compounds and ferrous metals. Additionally, testing will be required to determine exhaust plume size as well as leak rates in order to determine fair “stand-back” distances and inspection/maintenance frequencies to minimize risk to human health for astronauts at SCS and near the hop site.

## Main Engines

For the SLT to fulfill the range requirement, the SLT MEs must establish a significant thrust-to-weight ratio (TWR) in order to efficiently accelerate the craft to its suborbital trajectory without incurring significant gravity losses. The Apollo Lunar Module was used as a guideline for choosing an appropriate TWR; since it had an initial TWR of 2.124 [1], and the SLT will be unmanned, a TWR of double that of the Lunar Module was considered for the SLT. Therefore, assuming a maximum mass of 2000 kg (with  $g = 1.62 \text{ m/s}^2$ ,  $\therefore F_g = mg = 3240 \text{ N}$ ), engine configurations with a total thrust of 14 kN were desired.

Unfortunately, for the desired range, few engines were available to research in the public domain. However, several apogee engines exist in the 3-5 kN range, as well as larger engines in the 20 kN range; the implementation of these two types of engine configurations were analyzed in a trade study. The engine configurations were scored based on five traits: Thrust output,  $I_{sp}$ , controllability (thrust vectoring, etc.), and a size factor inversely proportional to engine dry mass. As shown in Appendix B, the quad-engine design using the DASA S3K engine was awarded the most points, primarily due to its very high  $I_{sp}$  allowing for greater  $\Delta V$  potential (and therefore greater range per pound of propellant). Technically, the S3K engine operates using mixed oxides of nitrogen (MON), specifically MON-3, which consists of 97% NTO with 3% nitric oxide ( $\text{NO}_2$ ) by weight; however, for simplicity the oxidizer is referred to as NTO.



Figure 27. CAD render of the SLT, showcasing the four main engines.

Stats for the S3K engine are given in the following table [18]:

<b>Property</b>	<b>Quantity (units, if app.)</b>
Dry Mass	14.5 kg
Length	1030 mm
Diameter	530 mm
Engine Cycle	Pressure-fed
Oxidizer	MON-3
Fuel	MMH
Thrust	3500 N
$I_{sp}$	352 s
Mixture Ratio	1.6-2.1
Chamber Pressure	9-12 atm

The engine chosen operates using a pressure-fed design; this is much preferred over a blowdown-type propellant feed system due to its much higher efficiency; the exorbitantly higher residual fuel inherent in blowdown designs makes them not worth considering in propellant selection; though not explicitly tested, it is improbable that a blowdown design could provide the required range capability while remaining under the maximum wet mass requirement. For pressurant, GHe is chosen over gaseous nitrogen, as the engine was designed to use GHe.

Regarding exhaust plume, simulations will also need to determine the magnitude and effects of lunar regolith ejection caused by the main engines. During liftoff and landing, 2 out of 4 engines may be deactivated in order to minimize regolith ejection; the efficacy of this strategy, as opposed to reduced throttle, may be examined during propulsion testing. Additional research

into the abrasive damage caused by long-term exposure to lunar regolith will be addressed during testing to determine any necessary inspection/maintenance routines related to regolith damage.

### ACS Thrusters

As mentioned above, only ACS thrusters compatible with MMH/NTO were examined. Due to the relatively small size and simplicity of ACS thrusters, there is a wide volume of makes and models of thruster that are suitable for the SLT. However, the DST-12 thruster by Moog Space and Defense Group claims the highest performance available in an ACS thruster of this fuel type [4], so it was chosen without a trade study. The 22 N thrust output (44 N in couples) of the thruster is sufficient for generating attitude control moments about the SLT's center of gravity, especially considering the ample coast time of the flight pattern and the additional acceleration supplemented by reaction wheels. Other nearly-equivalent ACS thrusters provided by Moog include the DST-13 and the "5 lbf" thruster; like the main engines, the main advantage of the DST-12 over its competing siblings is its superior  $I_{sp}$  of 302 seconds, as well as its slightly smaller length and mass:

	DST-12	DST-13	5 lbf
Thrust (N)	22	22	22
Mass (kg)	0.64	0.68	0.91
Length (mm)	244	264	343
$I_{sp}$ (s)	302	298	292

### Propellant Tanks

Similar to the ACS thruster selection process, due to the long heritage of MMH/NTO propellant, suitable propellant storage systems are in large supply. Titanium-alloy tanks were chosen due to their high strength-to-weight ratio for metallic propellant storage tanks. The volume of the tanks was chosen based on the required wet mass determined by  $\Delta V$  calculation as detailed in the following subsection; two 700L tanks (one each for fuel and oxidizer) manufactured by ArianeGroup, model OST 22/X, provide ample volume for propellant, including residual/unusable propellant; their maximum expected operating pressure also exceeds line and chamber pressures by a significant margin [2]:

Surface Tension Propellant Tank OST 22/X	
Tank Net Volume Range	700 to 1108 Litres
Propellants	MON respectively MMH
Geometrical Shape	Cassini Domes with variable cylindrical intersections
Maximum Expected Operating Pressure (MEOP)	19.5 bar
Proof Pressure (1.25 x MEOP)	24.38 bar
Burst Pressure (1.5 x MEOP)	29.25 bar
Interface Fixation	24 Suspension Tabs with floating nuts M8 x 1 (e.g.)
Materials	
- Pressure Vessel	Ti6Al4V STA (3.7164.7)
- Suspension/Ports	Ti6Al4V (3.7164.1)
- PMD	Ti99.4 (3.7034.1) and Ti6Al4V (3.7164.1)
- Screens	304L (1.4306); qualified also for Ti99.4 (3.7025.1)
Tank Mass Range	36 to 49 kg
Project Involvement	Artemis, Arabsat 2, Cesasat, Eutelsat W24, Arabsat BSS, Thaicom 3, Sinosat, Sirius

Figure 28. Propellant tank specifications, as provided by ArianeGroup.

As for pressurant storage, Northrop Grumman supplies several sizes of composite overwrapped pressure vessels (COPVs) for storing gases under high pressure. These consist of a fluid-retention liner wrapped in carbon fiber and offer the best strength-to-weight in their class. A single 81.4 L COPV (model number 80436) was used to pressurize each fuel and oxidizer tank [3].



Figure 29. A selection of Northrop Grumman COPVs.

## Trajectory

The SLT is required to demonstrate a capability of travelling 300 kilometers across the Lunar surface and back; this range requirement indirectly requires a total  $\Delta V$  requirement, in order to propel the craft from SCS to a remote location and back. However, without sophisticated trajectory simulations, in order to determine an appropriate propellant load, liberties must be taken

in representing a hypothetical flight path and fuel expenditure as accurately as possible without advanced tools.

A solution to this problem was found in blending a known overestimate of required  $\Delta V$  with a known underestimate; since the relationship between required  $\Delta V$  and range is strictly increasing (i.e., an increase in fuel expenditure always leads to an increase in range; this is known via Tsiolkovsky's ideal rocket equation), it can be inferred that the actual required  $\Delta V$  of the SLT must lie between two simple flight paths: one that *minimizes* gravitational losses, and another that *maximizes* gravitational losses. Creating these two flight paths is much more easily accomplished than creating a hyper-realistic simulated trajectory.

The two flight paths discussed above are: the absolute minimum  $\Delta V$  requirement to travel between two points on a spherical surface, determined via a minimum-energy ellipse; and a flight path which maximizes gravitational loss on ascent via a semi-rectangular trajectory. These paths are illustrated in the following figure:

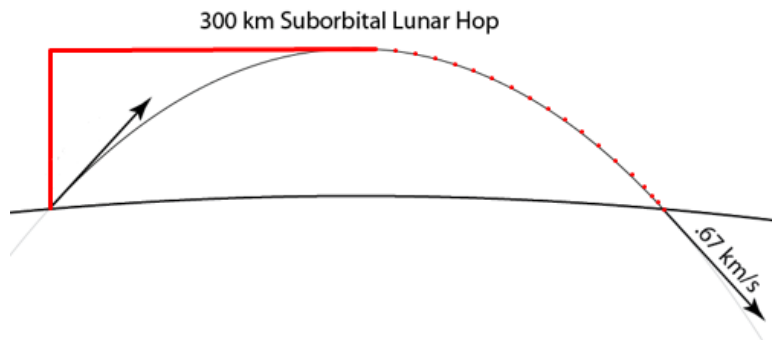


Figure 30. 300-kilometer suborbital lunar hop. Black shows the minimum-energy ellipse trajectory, while red shows the semi-rectangular trajectory.

As shown, the minimum-energy ellipse trajectory requires an initial, instantaneous velocity of 670 m/s; doubling to account for deceleration, then doubling again for the return trip yields a total  $\Delta V$  of 2680 m/s. The semi-rectangular trajectory requires more complicated math to account for gravitational losses, but yields a round-trip conservative  $\Delta V$  of ~4100 m/s. Due to the fact that the SLT possesses a high TWR, paired with the trajectory not accounting for TWR increase due to propellant mass loss, it can be fairly assumed that a propellant mass of 1350 kg (yielding a mass fraction of ~61%), and associated true  $\Delta V$  potential of ~3300 m/s, allows the SLT to perform the 300 km round-trip.

Additionally, the SLT is required to deorbit from an NRHO after insertion via the SLS CPL. However, this is calculated simply to be 2750 m/s: orbital energy calculations yield approximately 750 m/s  $\Delta V$  to transfer from NRHO to LLO, and another 2000 m/s to the surface. Gravitational losses were ignored, as the deorbit  $\Delta V$  is approximately equal to the hop  $\Delta V$ .

## Valving

Several references were consulted for proper valving components and placement. Below is a schematic of the relative location of each propulsion subsystem and any components associated with flow control to/from each subsystem. Total quantities of valving components are provided in the following subsection.

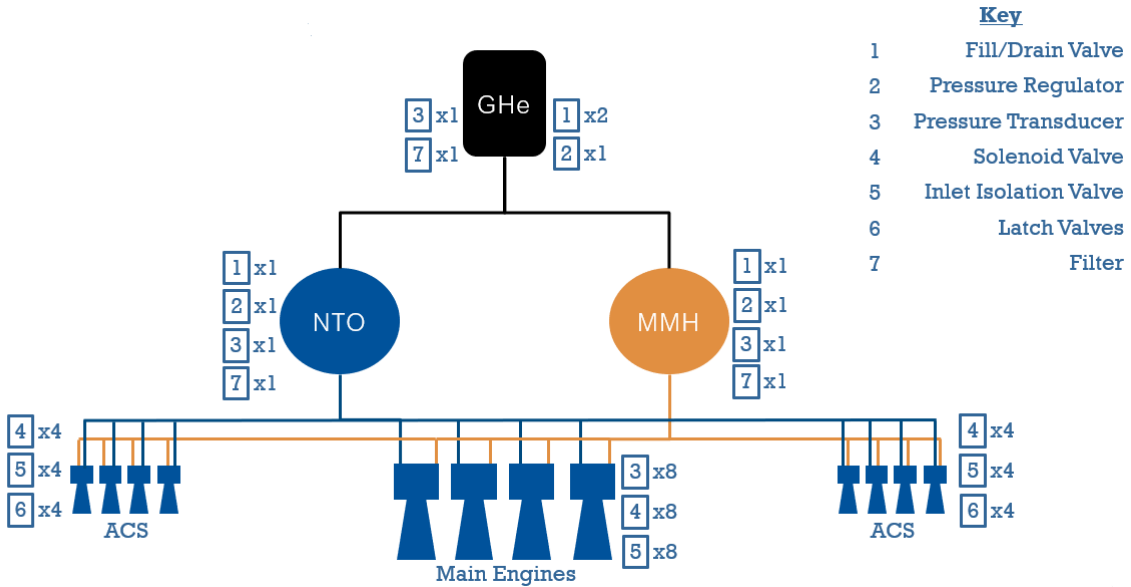


Figure 31. Propulsion Schematic. Refer to the key for component quantity and location.

## Cost

Total cost of the propulsion system for the SLT is divided into valving and non-valving categories, and listed below. See [7]-[17] for more information. The total cost of the propulsion system comes out to just over \$7 million.

### Valving Cost Information

As shown on the following page, total cost for valving comes to just under \$0.4 million.

Item	Quantity	Price (\$/ea.)	Cost (\$)	Supplier
Fill/Drain Valves*	5	1,500.00	7,500.00	Moog
Pressure Regulators*	3	4,000.00	12,000.00	Moog
Pressure Transducers*	11	5,000.00	55,000.00	Honeywell
Solenoid Valve	18	7,500.00	135,000.00	Triton Space
Inlet Isolation Valves*	16	7,500.00	120,000.00	Moog
Latch Valves*	8	4,000.00	32,000.00	ArianeGroup
Filter*	3	10,000.00	30,000.00	Mott
Check Valve*	12	500.00	6,000.00	Cobham
<i>*estimated</i>			<b>397,500.00</b>	

### Non-Valving Cost Information

As shown, the cost of all non-valving propulsion components totals to approximately \$6.6 million.

Item	Quantity (unit)	Price (\$/unit)	Cost (\$)	Supplier
MMH, bulk	947.8 lb	146.54	138,890.61	Department of Defense, Defense Logistics Agency
MON-3, bulk	1,990.3 lb	151.93	302,386.28	DoD DLA
GHe	0.0841 m <sup>3</sup>	33.21	2.79	DoD DLA
S3K Engine*	4	1,000,000.00	4,000,000	ArianeGroup
DST-12 Thruster*	8	250,000.00	2,000,000	Moog
Propellant Tank*	2	75,000.00	150,000.00	ArianeGroup
Pressurant COPV*	1	50,000.00	50,000.00	Northrop Grumman
Piping*	--	5,000.00	5,000.00	McMaster-Carr
<i>*estimated</i>			<b>6,646,000</b>	

## Risk Assessment

Risk assessment is done via the traditional probability-severity risk matrix method and illustrated in the following table. As shown, the only two catastrophic failures to potentially occur in the propulsion system are: propellant combustion backflow, an inherent flaw in liquid combustion engines; and total engine failure, an extremely unlikely occurrence. Due to the multiple engine design, total engine failure is even more unlikely, and a partial engine failure where only one or possibly two engines fail may not cause loss of mission.

Probability	Severity				
	1	2	3	4	5
5	Combustion product (soot) accumulation				
4					
3	Seal failure: leak (Pressurant)				
2			Seal failure: leak (propellant)	Valve failure: stuck open/closed	Propellant combustion backflow
1				Partial engine failure	Total engine failure

# Guidance and Navigation

## Overview

The GNC system has been divided into three subsystems: typical flight operation, descent and landing, and vehicle health. These subsystems will be described in further detail in the sections below. The typical flight subsystem is composed of star trackers, sun sensors, IMUs, reaction wheels, ACS thrusters, and flight computers. The descent and landing subsystem is composed of cameras, altimeters, IMU, NDL, HDL, reaction wheels, ACS thrusters, and a descent computer. The vehicle health subsystem is composed of a fuel sensor along with fuel estimation methods. The ACS thrusters have been discussed previously in the propulsion section. Utilizing all these components, the SLT will be capable of landing within 10 m precision, while avoiding hazards and dangerous landing sites.



Figure 32: Typical Flight components (from left to right) star tracker, sun sensor, IMU, reaction wheel, flight computer.

## Typical Flight Operation

As stated above, the typical flight subsystem is composed of star trackers, sun sensors, IMUs, reaction wheels, ACS thrusters, and flight computers. The star trackers and sun sensors determine position and orientation, the IMU determines linear motion and rotation, the reaction wheels and ACS thrusters correct the SLT's orientation, and the flight computer handles all data processing and commands. The total mass of this subsystem is 25 kg, total power draw is 409 W, and total cost is \$726K. Due to being over the mass requirement at PDR, one goal was to cut down on mass wherever possible. The power draw at PDR was also quite high, so this was cut down as well. The mass from PDR to CDR was reduced by 58% while power was reduced by 52%. Nearly every component was changed out besides the sun sensor, reaction wheels, and fuel sensor.

Three star trackers will be used; two are required to obtain a full view of the sky, while the extra will serve as backup in case of failure. The star tracker selected is the Arcsec Sagitta Star Tracker, as shown in the figure above. This component was selected through a trade study and was selected primarily due to its low mass and power consumption [1]-[7]. All trade studies discussed can be found in Appendix B. Eight sun sensors will be used, four to obtain a full view of the sky and four to serve as backups in case of failure. The sun sensor selected through a trade study is the

NewSpace Systems Fine Sun Sensor shown in Fig. 32 [8]-[12]. This sensor was selected due to its low mass and high accuracy. Two IMUs will be used, one functioning and one serving as backup. The IMU selected is the Epson M-G370PDS0; this was also selected through a trade study [13]-[16]. This component was also selected due to its low mass and high accuracy. Four reaction wheels will be used, one for each axis and one as backup. The reaction wheel selected through a trade study is the Honeywell HC9 [17]-[20]. This reaction wheel was chosen due to its high torque and momentum. Two flight computers are used simultaneously to satisfy redundancy. The flight computer chosen is the SEAKR Athena-3, which was selected through a trade study [21]-[24]. Since each component is either in a redundant configuration or has a backup in case of failure, the need for redundancy has been clearly met. Not only that, but certain components can be substituted for others. The sun sensors and star trackers can perform the same functions, so can the ACS thrusters and reaction wheels. The block diagram below illustrates the flow of commands throughout this subsystem. Note that everything can be remotely controlled at SCS if desired.

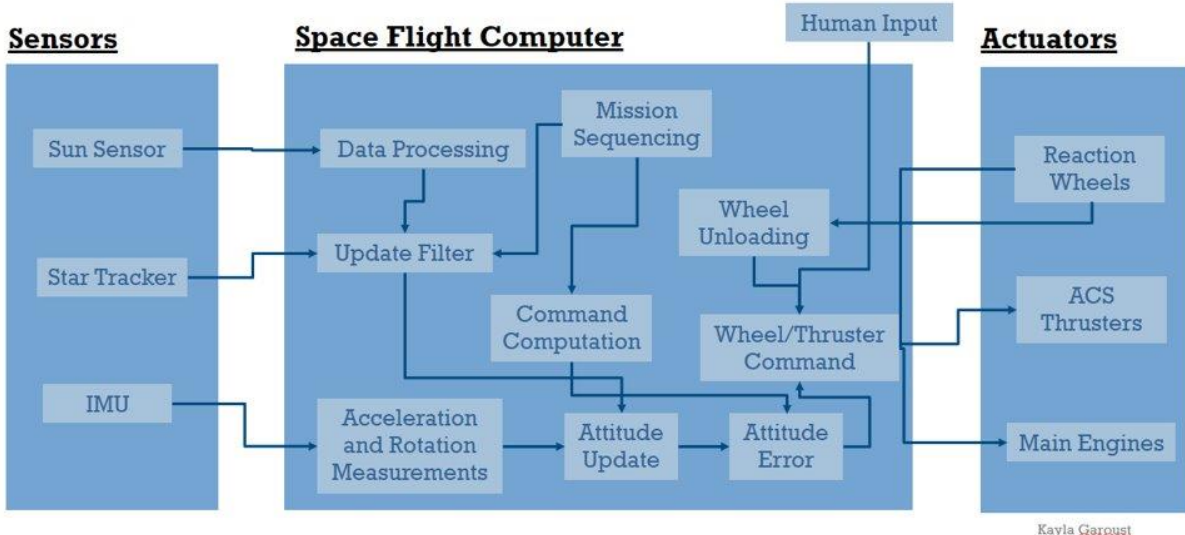


Figure 33: Block diagram showing flow of commands in typical flight operations.

## Descent and Landing

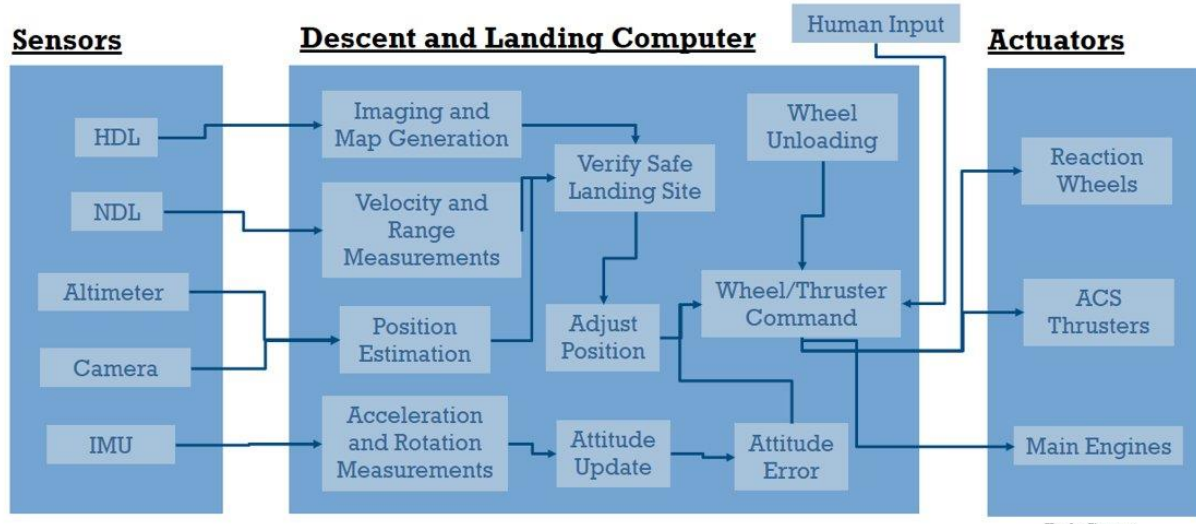


Figure 34: Descent and Landing components (from left to right) cameras, altimeter, HDL, NDL.

The Descent and Landing subsystem is composed of almost entirely SPLICE components, with the exception of the IMU, reaction wheels, and ACS thrusters. There is an additional Epson M-G370PDS0 IMU solely used while the SLT is in descent. This IMU could serve as a backup in case one of the flight IMUs malfunctions or vice versa. No additional reaction wheels or ACS

thrusters are used in Descent and Landing. The total mass of this subsystem is 90 kg, the total power draw is 265 W, and the total cost is \$1 million.

The SPLICE components consist of the cameras, altimeter, HDL, NDL, and descent and landing computer. SPLICE is a NASA founded technology that enables spacecraft to autonomously determine a safe landing site and then safely land there. The SPLICE technology will be capable of landing within 10 m accuracy by 2030. The cameras are used in TRN and will take photos of the moon's surface while the vehicle is searching for a safe landing spot and compare these images to stored images of the moon. A total of 10 cameras are used, with 3 of these serving as backups. At 6.4 km from the moon's surface the altimeter will activate and take range measurements. Two altimeters are used, with one being a backup. The NDL will also activate and begin taking velocity measurements. 500 m from the moon's surface the HDL will activate and begin scanning for hazards to secure a safe landing spot. The descent and landing computer will be handling all data processing and commands during descent. In case of computer malfunction or failure one of the flight computers could take over for the descent and landing computer or vice versa. The flow of commands within this subsystem is illustrated in the diagram below, and again can be remotely controlled at SCS if desired.



Kayla Garousi

Figure 35: Descent and Landing block diagram showing flow of commands.

## Vehicle Health

The vehicle health subsystem's function is to determine the amount of fuel remaining to determine mission life, as well as recalculate the SLT's center of gravity for inertial measurements. A trade study was performed on the various methods of estimating remaining fuel in spacecraft, and it was found that bookkeeping the simplest and most efficient method for doing so [25], [26]. Bookkeeping is the method of determining the fuel remaining based on the duration of burns and

subtracting the fuel expended. However, the errors in calculations from bookkeeping accumulate over time, so to counter this, ECVT fuel sensors will also be used. ECVT is a new technology and not much is known at this time, which is why bookkeeping will be the primary method and ECVT will be secondary. The current accuracy of ECVT fuel sensors is less than 6%, while the error in bookkeeping calculations can be as high as 10%. By using these two methods simultaneously, more accurate calculations will be obtained and the need for redundancy is met.

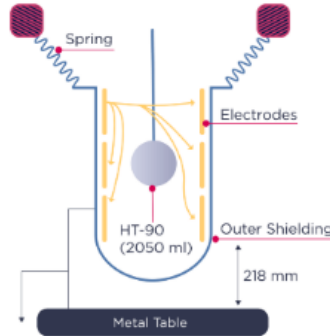


Figure 36: ECVT fuel sensor

## Risk Assessment

A risk assessment was performed on the entire GNC system and is shown in the figure below. Due to all the redundancy and backup components, the majority of failures are minor and can be ignored due to their low severity or low likelihood. The main concerns found are the NDL and HDL not having backup components. Due to their sheer size and mass only one of each component is used, however the likelihood of either of these failing is not high enough to cause concern.

Probability	Severity				
	1	2	3	4	5
5	Cameras malfunction				
4	One reaction wheel fails		Bookkeeping calculations are incorrect		
3	One star tracker fails	One IMU fails			

		50% of the sun sensors fail Two reaction wheels fail	Two startrackers fail Two IMUs fail	ECTV fuel gage malfunctions Computer failure	Two altimeters fail
1			100% of the sun sensors fail Three IMUs fail	Three star trackers fail Three reaction wheels fail	NDL fails HDL fails

Figure 37: Risk assessment of the GNC system.

# Communications

## Overview

The communications system onboard the SLT is capable of both X-band and S-band communications, as these are the primary radio frequencies used in spaceflight. The system is composed of an SDR, antennas, and amplifiers, as shown in the figure below. Two SDRs are used, having one as backup. The SDR selected is the Blue Canyon Technology's SDR. This component was selected through a trade study [1]-[4]. There are two X-band antennas used, one as backup. The EnduroSat X-band Antenna was selected through a trade study [5]-[8]. Two S-band antennas will be used as well, with one being backup. The S-band antenna selected is the ISISpace S-band antenna, which was selected through a trade study [7]-[10]. For each band of communication, two amplifiers are used, with one backup per band. The X-band amplifier selected is the Qorvo TGM2635-CP. The S-band amplifier selected is the Pasternack PE15A5003. These were both selected via trade study [11]-[18].

Due to the SLT being over the mass requirement at PDR, it was necessary to reduce mass wherever possible. The total power draw at PDR was also high and it was desired to reduce this as well. The total mass reduction in this system between PDR and CDR was 95%. The current total mass of this system is 0.6 kg. The power reduction from PDR to CDR was 72%. The power draw from this system is now 50 W. The total cost of this system is \$92K. The components that changed from PDR to CDR were the SDR and amplifiers. A transponder was also removed from the design due to it being found that having one was not necessary. Some future changes to keep in mind would be upgrading the antennas. Currently all the antennas are patch antennas and do not have as high of a gain as deployable antennas. If higher gain communications were desired in the future, these patch antennas could be upgraded to deployable antennas. The SDR selected is capable of X-, S-, and Ka-band communication, so to make the entire system capable of Ka-band communication, Ka-band antennas and amplifiers could be added to the SLT if desired.

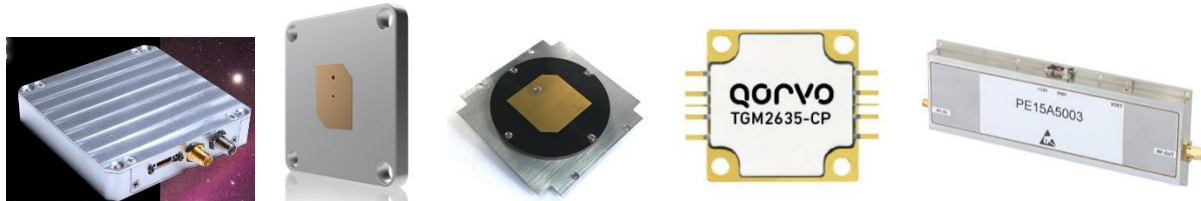


Figure 38: Communications components (from left to right) SDR, X-band antenna, S-band antenna, X-band amplifier, S-band amplifier.

## Risk Assessment

A risk assessment was performed on the communications system and is shown in the figure below. Due to every component having a backup, there are not too many areas of concern on the

risk assessment. The biggest issue would be an error in receiving communications. Receiving the correct information is vital to the mission, as well as communicating back. There is the potential for the SLT to become lost or unable to communicate with SCS. Although, the likelihood of this is low, it is still something to keep an eye on.

Probability	Severity				
	1	2	3	4	5
5					
4					
3					
2		Antenna failure Amplifier failure	SDR failure	Communications not received properly	
1					Communications not encrypted

Figure 39: Risk assessment of the communications system.

## Environmental

### Thermal

#### Thermal Environments and Requirements

The SLT would deal with a large range of thermal environments during its operational life including before its launch. A table of temperature highs and lows has been made with the temperature environments on the moon being the last row. As can be seen, the environments in the lunar highlands far overshadow the other environments the SLT would exist in.

Environment	Temperature Low (°C)	Temperature High (°C)
SLS Rollout	-1	41
SLS On-Pad Unfueled	12	39.4
SLS On-Pad Fueled	1.1	38.3
SLS Launch to Core Separation	-2.2	31.7
SLS Core Stage Separation to SEC01	-7.2	32.2
SLS SEC01 to ORION Separation	-68.9	33.33
SLS ORION Separation to USA Jettison	-76.7	30
SLS Orbital Environment as CPL with ORION	11	55
Lunar Highlands	-250	120

Figure 40 [1] [2]

The SLT would have to exist 72 hours in the lunar night conditions and as a CPL on the SLS, would have to survive around 6 days during transit to the moon.

As for the components on board, the SLT would have to account for a wide range of thermal requirements. A table of such requirements has been put together below. Components such as the star trackers and flight computers require lower temperatures and can put off too much heat for them to deal with. On the other hand, both propellants have tight requirements to stay in their liquid phases and would need to be kept both cooled and heated.

Item	Temperature Low (°C)	Temperature High (°C)
MMH Fuel	-52	87
MON-3	-15	20
Payload Compartment	0	40
Batteries	0	30
Navigation Components (Star tracker, Sun Sensor, etc.)	-30	50

Figure 41 Thermal requirements of onboard requirements

## Thermal Control

A single-phase fluid loop system based on the heat rejection system on board Mars Pathfinder, capable of routing excess heat from high temperature components to low temperature components. Components were decided through trade studies prioritizing thermal conductivity and operational temperature range. The full study can be found in Appendix B.

The system would use Fluoronert FC-40 as a medium to transport heat from electric heaters and hot components such as the flight computer to either components that need to be warmed such as the propellant and batteries or, if necessary, to a silver and Teflon coated aluminum radiator to be removed. The system would have a mass of 35.1 kg. And would have to be able to reject up to 2,056 W of heat in a worst case, hot situation.

In addition, to reject solar radiation, an 18-layer MLI would be used, having an Aluminized Beta cloth outer layer, aluminized Kapton reflective layers, and Dacron netting spacing the reflective layers. This system was designed to reflect 86.5% of solar radiation which would otherwise impart around 5440 W of heat to the craft. The specifications of the MLI is outlined in the table and graph below. 18 layers was selected as, through absorption analysis, the number of reflective layers begins to have diminishing returns as more are added. 8 reflective layers provided a comfortable middle ground for the team.

MLI Layer	Material	Cost [\$/m^2]	Mass [g/cm^2]	Absorbtion	End of Life Emissivity	Thickness [mm]	Number of layers
Outer	Aluminized Beta Cloth	443.2	0.0271	0.37	0.3	0.2	1
Reflective	Aluminized Kapton	68.75 <a href="#">[Link]</a>	0.019	0.12	0.05	0.127	8
Spacer	Dacron Netting	75	0.00063	-	-	0.16	9

Figure 42 MLI Specifications [3]

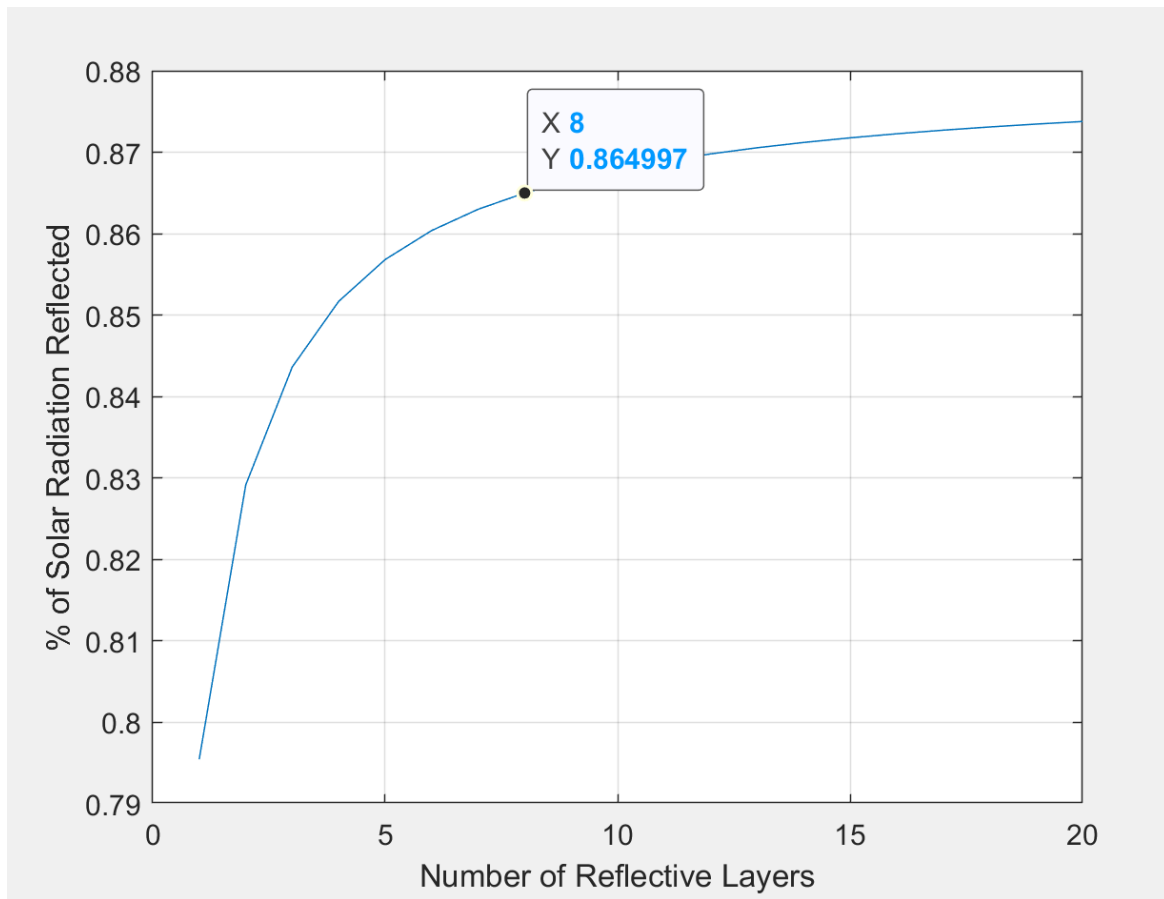


Figure 43: A graph of the solar reflectivity as a function of how many reflective layers are used on the craft

## **Thermal Concerns & Risk Management**

Many risks and concerns exist when it comes to the thermal control system. For example, the speed at which the SLT reacts to changes in temperature would need to be tested. However, many moderate to high level risks need to have plans in place to not risk the mission. These include but are not limited to:

- Multiple Layers of the MLI are damaged.
  - Patches of the MLI can be made that can be attached to the craft in the event of severe insulation damage.
- Electronics reject more heat than estimation resulting in overheating.
  - Pre-launch testing of components should alleviate this issue.
- Coolant leak from heat pipes.
  - Extra coolant will need to be kept at SCS.
  - Heat pipes would need a modular design to allow for easy switching of parts.
- Damage to radiator.
  - When not in operation, a cover can be placed over radiator. In addition, strict guidelines would need to be followed during construction.
  - On earth a new radiator would need to be constructed. In lunar operation this would ground the vehicle until a replacement could be created.

## **Vibroacoustic**

### **Vibroacoustic Environments**

As part of the payload on the SLS the SLT will deal with powerful vibroacoustic loads during takeoff as the SLS burns its fuel. These would especially be powerful during the period of maximum dynamic pressure. As for low frequency vibrations, the SLT would experience random vibrations starting at 27 Hz with increasing intensity until a frequency of 60 Hz. As for high frequency acoustics, the SLT would have to deal with frequencies across a large range with a total sound level of 144.7 dB. A table of the vibration and acoustic environments can be found below. These were provided by the SLS Mission Planner's Guide provided by NASA. However, the SLT will experience vibrations from its own engines too during normal mission operation. Unfortunately, the specifics of the environment caused by the engines is unknown and would have to be found during testing. This provided a unique challenge as any control system would have to be designed to be rigorous enough to protect against a wide range of frequencies.

**Table 5-18. CPL Vehicle Dynamics Criteria**

Frequency (Hz)	Normal		Frequency (Hz)	In Plane	
	Input (g)	Slope (dB/Octave)		Input (g)	Slope (dB/Octave)
5	0.22		5	0.22	
20	0.22		22	0.22	
27	0.26	2.15	31	0.31	
35	0.26		60	0.31	4.23
60	0.16	-4.92			

*Figure 44 Vibration environments on SLS [2]*

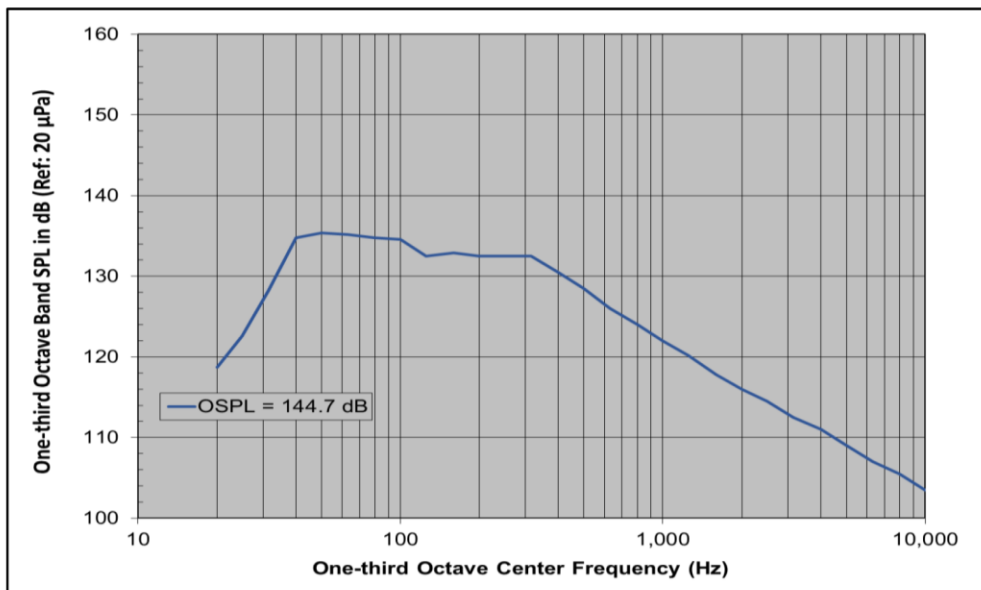


*Figure 45 Acoustic environment onboard SLS [2]*

### Vibroacoustic Control

To control low frequency vibrations, 3 Moog Shockwave Dampers would be used to isolate any electronics and to isolate the engines from the rest of the SLT. These are tuned mass dampers which are designed to isolate 20 Hz frequencies [4]. By placing these in parallel, the dampers can damp a peak frequency of 60 Hz while still being rigorous enough to deal with a range of frequencies in the event of a change in behavior due to a change in design. In addition, this would allow for the unknown frequencies from the onboard engines to be dealt with. This device was chosen based on a trade study focusing on mass and size as many would have to be used. This trade study can be found in Appendix B. In total, 15 dampers would be used which would have a total mass of 1.2 kg.



Figure 46 Side image of the Moog Shockwave Damper

As for high frequency acoustics, a 2-inch (50.8 mm) layer of flat faced melamine foam would be used to cover any sensitive parts of the SLT such as its sensors. In addition, to protect the SLT during takeoff, a shell would be formed around the craft while it sits in the payload bay. This shell would be 36 square meters and would have a mass cost of 17kg and a cost of around \$500. This foam was decided through a trade study prioritizing density and the absorption coefficients at 1 kHz and 2 kHz. [5]



Figure 47 Isometric image of the melamine foam

### **Vibroacoustic Concerns & Risk Management**

Many of the vibroacoustic concerns are related to changes in the frequency of vibrations. Whether this be through a change in the structure of the craft which causes a change in the craft's resonant frequency, or through a change in the engines causing a change in the vibration environment. However, many if not all the concerns would be solved through thorough testing of the craft and all its components before manufacturing.

# Electrical

## Overview

The electrical system is comprised of a power source, power storage, PMAD, and cable. The total mass of this system is 27 kg, the total power produced is 30 kW, and the total cost is \$650K. The only electrical actuators used in the SLT are for the PDM design and are discussed in the mechanisms section. For the power source, a trade study was performed, and it was found that using solar is the best power option for this mission [1]. A trade study was then performed to select the specific solar panels and the Redwire Space ROSA was selected [2]-[5]. These solar panels were selected based on their high power and simplicity. The ROSA deploys using its own strain energy, so no motors or complex mechanisms are needed. Lithium-ion batteries are used as the power storage for the SLT based on research. A trade study was performed to select the batteries and the EaglePicher SLC-21060-003 was selected as the battery [6]-[9]. A total of 10 batteries will be used, providing almost 3 kWh of power when fully charged. For PMAD, another trade study was performed and the AAC Clyde Space Starbuck Mini was chosen [10]-[13]. Two of these components will be used simultaneously, enabling power management of up to 3 kW.



Figure 48: Electrical components (from left to right) solar panels lithium-ion battery, PMAD.

## Inventory

The figure below shows the list of all components requiring power and the power consumption of each one. The quantity of each component used in the table is based on components actually in use and does not include backups.

Subsystem	Component	Quantity in Use	Nominal/Peak Power [W]	Total Peak Power [W]
GNC	Star Tracker	2	1.4	2.8
GNC	Sun Sensor	4	0.015/0.15	0.6

GNC	IMU	1	0.05	0.05
GNC	Reaction Wheels	3	5/130	390
GNC	Flight Computer	1	16	16
GNC	Cameras	7	2/5	35
GNC	Altimeter	1	5/10	10
GNC	NDL	1	85	85
GNC	HDL	1	85	85
GNC	Descent Computer	1	20/50	50
Comms	SDR	1	1.8	1.8
Comms	S-band Antenna	1	2	2
Comms	S-band Amplifier	1	5	5
Comms	X-band Antenna	1	4	4
Comms	X-band Amplifier	1	5	5
Enviro	Thermal Control	1	33%	33%
Electrical	PMAD	2	20	40
Propulsion	Pressure Regulators	3	4.4	13.2
Propulsion	Pressure Transducer	11	3.2	35.2
Propulsion	Solenoid Valve	10	857	8,570
Propulsion	Inlet Isolation Valve	16	448	7,168
Propulsion	Latch Valve	8	167	1,336

Figure 49: Electrical items inventory.

## Power Requirements

The total peak power required by each system is shown in the table below. These totals were calculated based on the table above and summing the components of each system. The payload power requirement is given by the customer. This means that the power required during flight is 2.3 kW, and 2.1 kW during landing. While the SLT is on the ground running communications, payload support, thermal control, and computer functions the power required is

0.625 kW. It was also given that the SLT is required to survive 72 hours at lunar night. Multiplying the ground operation power required by 72 hours gives 45 kWh. Since solar panels will not work at lunar night, this power needs to come from the batteries. Also accounting for two flights and two landings and adding these to the 72-hour night power requirement, brings this to a total of approximately 47 kWh. Since each battery is capable of providing 0.26 kWh of energy, a total of 10 batteries will be used, providing 2.6 kWh of energy. It is also assumed that the solar panels are fully charged at the start of the mission, which will provide another 30 kW of energy. Utilizing 10 lithium-ion batteries, along with the solar panels, the 72-hour night requirement will be met.

System	Peak Power [W]
GNC – Typical Flight	409.45
GNC – Landing	265.05
Communications	50
Thermal	33% of total
Propulsion	857
Payload	420

*Figure 50: Tables containing power totals by system.*

## Cable Routing

In the figure below, the wiring configuration of the SLT is illustrated. All sensors, along with the payload are connected to the flight computer for commands and data handling. The computer is powered by the battery configuration, which is depicted as a single battery in the diagram below. The batteries are powered by the solar panels, once the batteries are at capacity the solar panels will remain fully powered until there is more room in the batteries. The PMAD will work alongside the flight computer in ensuring efficient power distribution and voltage monitoring.

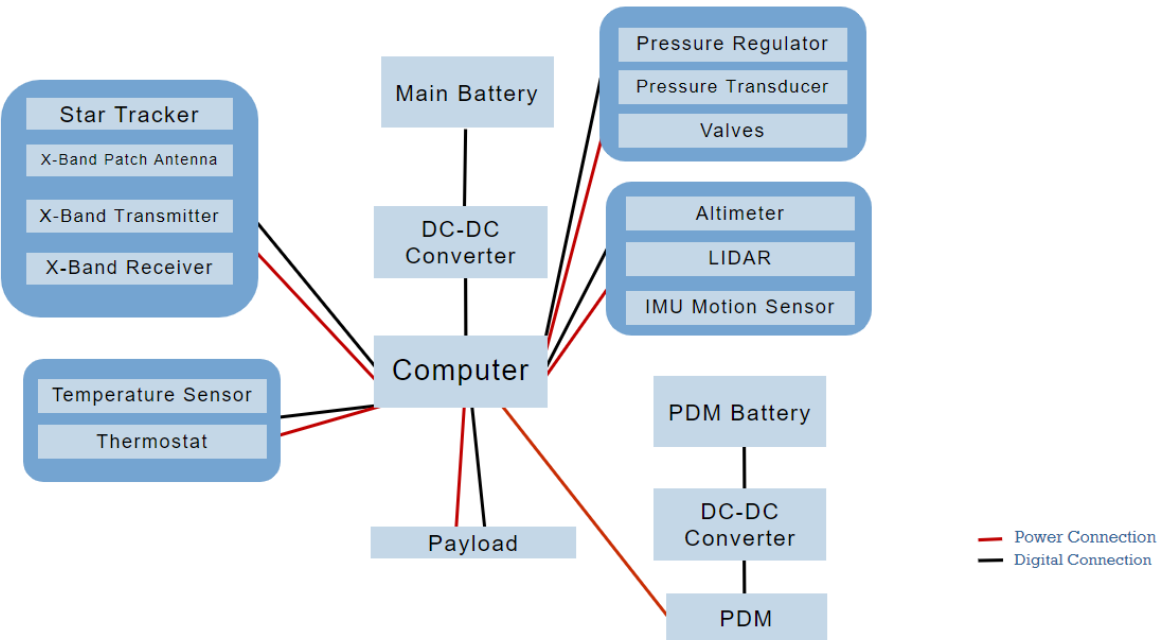


Figure 51: Diagram showing flow of power.

## Risk Assessment

A risk assessment was performed on the electrical system. Without having started testing, not much knowledge is available at this time. This risk assessment will be updated as testing progresses. The main concern in the figure below would be not having enough power supplied. Not having enough power could mean mission failure. The payload could malfunction or the SLT might be stranded without enough power to make the return flight. This will need to be further addressed in testing. Perhaps, more “buffer” is needed in the power requirements calculations to ensure the power provided is above and beyond the power needed.

Probability	Severity				
	1	2	3	4	5
5	Green	Yellow	Red	Red	Red
4	Green	Yellow	Yellow	Red	Red

3					
2			Solar panels fail to deploy	PMAD malfunction	Not enough power is supplied
1		Battery runs out			

Figure 52: Risk assessment of the electrical system.

# Testing

Testing must be meticulous to ensure the system is robust, reliable, and functions properly.

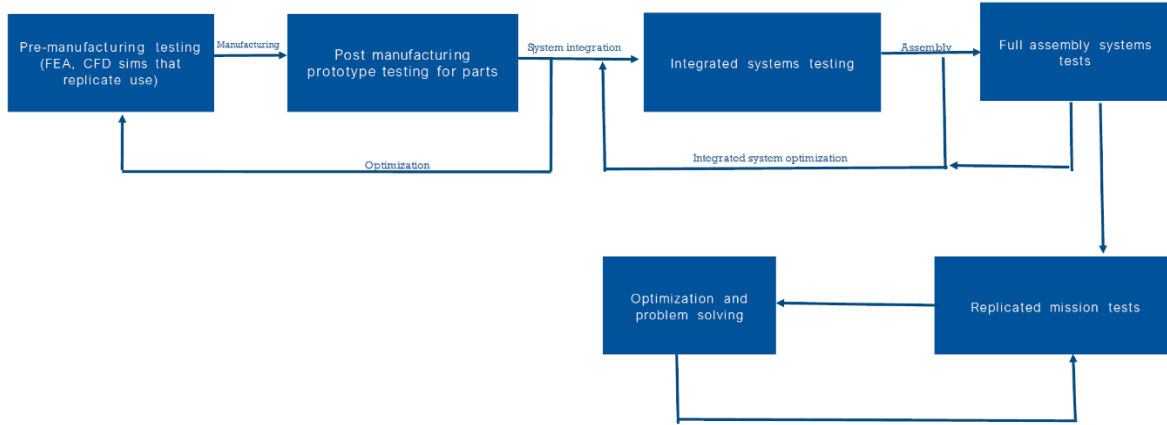


*Figure 53-Testing Plan of Action*

Each part will first be subjected to preliminary tests before they are manufactured that include FEA modelling, or any other relevant simulations. Once satisfied, the parts are manufactured, and individual component testing begins. As seen in the flow chart, parts are given the opportunity to be optimized and retested before they move on to the next phase of testing. For systems testing, the components are integrated into their respective systems and tested again. An optimization and retest period are also accounted for during systems testing. Once completed the systems are assembled into the full SLT where full assembly testing can begin. Here, all tests are run again and the SLT is optimized before moving on to replicated mission testing. Individual components will undergo vibration, sound, structural, electronic, and software tests. The systems test phase includes all the same tests with the addition of thermo-vacuum testing and propulsion testing. The full assembly testing includes every test with the edition of some replicated missions test. NASAs Johnson Space Center in Houston Texas will serve as our main testing facilities where testing for vibration, sound, structural, and thermo-vacuum testing will be conducted. All electronic and software testing will be conducted in-house to avoid a third-party testing company. All issues can be fixed, and the engineers can learn more about how the systems behave. Propulsion testing will take place in NASAs Marshall Space Flight Center.

A budget was put together using quotes given by Element Materials Technology to develop an estimate for how much testing would cost.

	Vibration		Vibroacoustic		Structural		Propulsion		Electronics		Software		Thermal vacuum		Mission Replication	
	# of tests	Cost \$	# of tests	Cost \$	# of tests	Cost \$	# of tests	Cost \$	# of tests	Cost \$	# of tests	Cost \$	# of tests	Cost \$	# of tests	Cost \$
<b>Small Scale</b>	200	20000	200	15000	200	15000	N/A	N/A	75	10000	50	10000	N/A	N/A	N/A	N/A
<b>Large Scale</b>	50	50000	50	40000	50	35000	40	65000	40	15000	40	15000	40	60000	10	70000
<b>Totals \$:</b>	<b>6500000</b>		<b>5000000</b>		<b>4750000</b>		<b>2600000</b>		<b>1350000</b>		<b>1100000</b>		<b>2400000</b>		<b>700000</b>	
<b>Final Total \$:</b>	<b>24400000</b>															

*Figure 54-Testing Budget (Estimate)*

There is some concern with testing. The budget needs further research to update into a more accurate model. There is also always a concern when working with hazardous materials and procedures. The goal of the testing procedure is to accurately model the environments in which the mission takes place. Some mission environments are extremely hard to replicate on Earth, especially the parking orbit at the mission start. More research and development should help alleviate these issues.

An in-depth schedule was made that detailed each test, assembly and disassembly, problem solving, retests, and transportation to and from facilities. It should also be noted that a 3 yearlong buffer period is also accounted for to deal with any issues and allow for ample time to fix any errors with the SLT and retest until we are sure that the SLT is reliable in all circumstances.

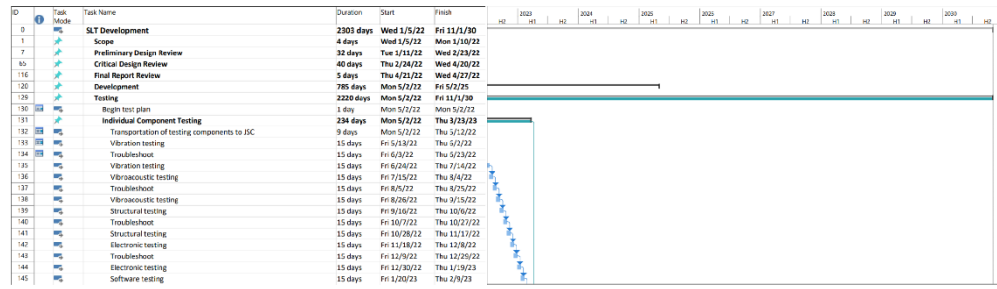


Figure 55-Testing Schedule 1

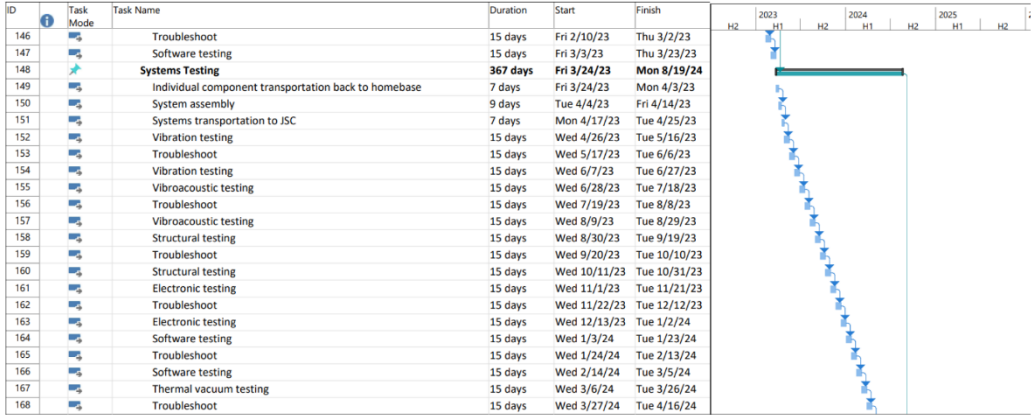


Figure 56-Testing schedule 2



Figure 57-Testing Schedule 3

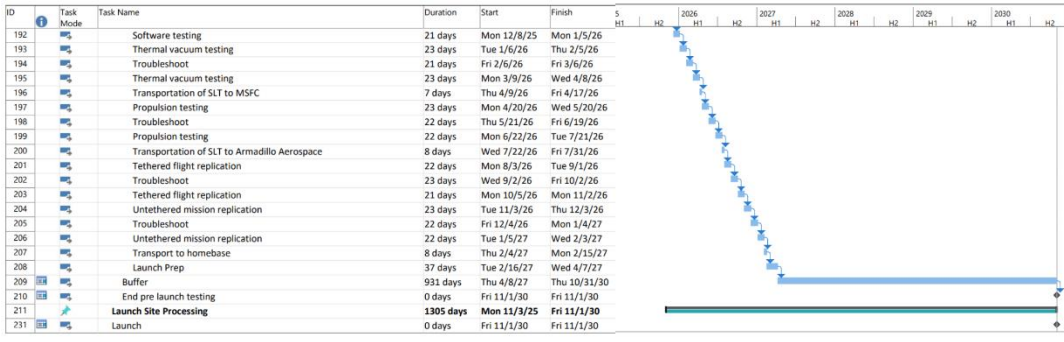


Figure 58-Testing Schedule 4

## References

### Structures

- [1] <http://www.totalmateria.com/Article23.htm>
- [2] [https://www.jstage.jst.go.jp/article/matertrans1960/28/10/28\\_10\\_773/\\_article](https://www.jstage.jst.go.jp/article/matertrans1960/28/10/28_10_773/_article)
- [3] <https://materialsdata.nist.gov/bitstream/handle/11115/177/Mecnanical%20Properties%20Data.pdf?sequence=3&isAllowed=y>
- [4] <https://grabcad.com/library/rs-25-rocket-propulsion-engine-on-solidworks-1>
- [5] <https://www.northropgrumman.com/space/pressurant-tanks/>
- [6] <https://satcatalog.s3.amazonaws.com/components/801/SatCatalog - ArianeGroup - 700 L Biprop Tank - OST 22-X - Datasheet.pdf?lastmod=20210709220745>
- [7] <https://stars.library.ucf.edu/cgi/viewcontent.cgi?referer=&httpsredir=1&article=2411&context=etd>
- [8] <https://grabcad.com/library/solar-panel-22>
- [9] <https://arc.aiaa.org/doi/abs/10.2514/4.861796>
- [10] <https://www.mt-aluminum.com/aluminum-7075-price-per-kg.html>
- [11] [https://tigerprints.clemson.edu/cgi/viewcontent.cgi?article=1020&context=mecheng\\_pubs#:~:text=The%20current%20constraint%20in%20using,steel%20and%20aluminum%20%5B6%5D.](https://tigerprints.clemson.edu/cgi/viewcontent.cgi?article=1020&context=mecheng_pubs#:~:text=The%20current%20constraint%20in%20using,steel%20and%20aluminum%20%5B6%5D.)
- [12] <https://www.toraycma.com/wp-content/uploads/M55J-Technical-Data-Sheet-1.pdf.pdf>
- [13] <http://asm.matweb.com/search/SpecificMaterial.asp?bassnum=mtp641>
- [14] <http://asm.matweb.com/search/SpecificMaterial.asp?bassnum=ma7075t6>
- [15] <http://asm.matweb.com/search/SpecificMaterial.asp?bassnum=MA7178T6>
- [16] <https://www.indiamart.com/proddetail/astm-b209-gr-7178-aluminum-sheet-11483775097.html>
- [17] [http://www.metalspiping.com/titanium-alloy-ti-6al4v.html#:~:text=Price%20for%20Ti%2D6Al%2D4V%20bar\(ASTM%20B348%20Gr,20%20per%20kg](http://www.metalspiping.com/titanium-alloy-ti-6al4v.html#:~:text=Price%20for%20Ti%2D6Al%2D4V%20bar(ASTM%20B348%20Gr,20%20per%20kg)
- [18] <https://wwwazonano.com/article.aspx?ArticleID=5365#:~:text=Engineers%20have%20found%20a%20solution,7075%20joints%20without%20hot%20cracks.>

## Mechanisms

- [1] [http://www.russianspaceweb.com/ptk\\_pu.html](http://www.russianspaceweb.com/ptk_pu.html)
- [2] chrome extension:// efaidnbmnnnibpcajpcglclefindmkaj viewer.html?pdfurl =https%3A%2F%2Fntrs.nasa.gov%2Fapi%2Fcitations%2F20070031904%2Fdownloads %2F20070031904.pdf&clen=1439226
- [3] chrome extension:// efaidnbmnnnibpcajpcglclefindmkaj viewer.html?pdfurl =https%3A%2F%2Fntrs.nasa.gov%2Fapi%2Fcitations%2F19690002490%2Fdownloads %2F19690002490.pdf&clen=473171
- [4] chrome extension:// efaidnbmnnnibpcajpcglclefindmkaj viewer.html?pdfurl =https%3A%2F%2Fjournals.sagepub.com%2Fdoi%2Fpdf%2F10.1177%2F17298814177 20467&pdffilename=1729881417720467.pdf
- [5] chrome extension:// efaidnbmnnnibpcajpcglclefindmkaj viewer.html?pdfurl =https%3A%2F%2Fltu.diva portal.org%2Fsmash%2Fget%2Fdiva%3A1159285%2FFULLTEXT01.pdf&clen=5443 553
- [6] [https://www.transmotec.com/product/kp5fn\\_22105\\_cvc/](https://www.transmotec.com/product/kp5fn_22105_cvc/)
- [7] [https://kawakaviation.com/what\\_we\\_do/electric\\_motors/bldc\\_electric\\_motors/](https://kawakaviation.com/what_we_do/electric_motors/bldc_electric_motors/)
- [8] <https://www.mcmaster.com/6627T103/>
- [9] <https://www.mcmaster.com/6627T102/>
- [10] [https://www.aegisbattery.com/collections/12v\\_14v\\_nmc\\_li\\_ion\\_batteries/products/28v\\_5ah\\_li\\_ion\\_battery\\_nmc\\_soft\\_pack\\_abl\\_028005p\\_1?variant=37800217903298](https://www.aegisbattery.com/collections/12v_14v_nmc_li_ion_batteries/products/28v_5ah_li_ion_battery_nmc_soft_pack_abl_028005p_1?variant=37800217903298)
- [11] [https://www.aegisbattery.com/products/28v\\_5ah\\_li\\_ion\\_battery\\_nmc\\_soft\\_pack\\_abl\\_028005p?variant=37800209547458](https://www.aegisbattery.com/products/28v_5ah_li_ion_battery_nmc_soft_pack_abl_028005p?variant=37800209547458)
- [12] chromeextension:// efaidnbmnnnibpcajpcglclefindmkaj viewer.html?pdfurl =https%3A%2F%2Fstars.library.ucf.edu%2Fcgi%2Fviewcontent.cgi%3Freferer%3D%2 6httpsredir%3D1%26article%3D2411%26context%3Ddetd&clen6035164&pdffilename=P ressurized%20Metal%20Bellows%20Shock%20Absorber%20for%20Space%20Applicati ons..pdf
- [13] [https://www.researchgate.net/publication/236035258\\_Design\\_and\\_Experimental\\_Ch aracterization\\_of\\_Electromagnetic\\_Shock\\_Absorbers\\_for\\_Landing\\_Gears](https://www.researchgate.net/publication/236035258_Design_and_Experimental_Ch aracterization_of_Electromagnetic_Shock_Absorbers_for_Landing_Gears)
- [14] chrome extension:// efaidnbmnnnibpcajpcglclefindmkaj viewer.html?pdfurl =https%3A%2F%2Fesmats.eu%2Fesmatspapers%2Fpastpapers%2Fpdfs%2F2011%2Fpo nnusamy.pdf&clen=578549&chunk=true

## Propulsion

- [1] <https://georgetyson.com/files/apollostatistics.pdf>
- [2] <https://www.space-propulsion.com/spacecraft-propulsion/bipropellant-tanks/index.html>
- [3] <https://www.northropgrumman.com/space/pressurant-tanks/>
- [4] [https://www.moog.com/content/dam/moog/literature/Space\\_Defense/spaceliterature/propulsion/moog-bipropellant-thrusters-datasheet.pdf](https://www.moog.com/content/dam/moog/literature/Space_Defense/spaceliterature/propulsion/moog-bipropellant-thrusters-datasheet.pdf)
- [5] <https://www.rocket.com/sites/default/files/documents/In-Space%20Data%20Sheets%204.8.20.pdf>
- [6] <http://hopsblog-hop.blogspot.com/2015/08/lunar-pogo-hopper.html>
- [7] [https://www.moog.com/content/dam/moog/literature/Space\\_Defense/spaceliterature/propulsion/moog-manual-fill-and-drain-valves-datasheet.pdf](https://www.moog.com/content/dam/moog/literature/Space_Defense/spaceliterature/propulsion/moog-manual-fill-and-drain-valves-datasheet.pdf)
- [8] [https://www.moog.com/content/dam/moog/literature/Space\\_Defense/spaceliterature/propulsion/moog-proportional-flow-control-valve-datasheet.pdf](https://www.moog.com/content/dam/moog/literature/Space_Defense/spaceliterature/propulsion/moog-proportional-flow-control-valve-datasheet.pdf)
- [9] <https://prod-edam.honeywell.com/content/dam/honeywell-edam/sps/siot/us/products/test-and-measurement-products/pressure-transducers/aerospace/model-as25d/documents/sps-siot-t-m-model-as25d-aero-diff-pressure-transducer-datasheet-008712-1-en-ciid-151986.pdf>
- [10] [https://www.moog.com/content/dam/moog/literature/Space\\_Defense/spaceliterature/propulsion/moog-bipropellant-thruster-valves-datasheet.pdf](https://www.moog.com/content/dam/moog/literature/Space_Defense/spaceliterature/propulsion/moog-bipropellant-thruster-valves-datasheet.pdf)
- [11] <https://www.triton-space.com/blog/tag/Rocket+propulsion+valves>
- [12] [https://www.moog.com/content/dam/moog/literature/Space\\_Defense/spaceliterature/propulsion/moog-pilot-operated-isolation-valve-datasheet.pdf](https://www.moog.com/content/dam/moog/literature/Space_Defense/spaceliterature/propulsion/moog-pilot-operated-isolation-valve-datasheet.pdf)
- [13] <https://www.space-propulsion.com/spacecraft-propulsion/valves/latch-valve.html>
- [14] <https://mottcorp.com/wp-content/uploads/2022/01/Mott-Propellant-Filters-Rev-0122.pdf>
- [15] <https://www.cobhammissionsystems.com/space-propulsion-systems/propulsion-check-and-relief-valves/propulsion-check-and-relief-valves-datasheet/docview/>
- [16] [https://www.dla.mil/Portals/104/Documents/Energy/Standard%20Prices/Aerospace%20Prices/E\\_2017Oct1AerospaceStandardPrices\\_170913.pdf?ver=2017-09-13-145335-477](https://www.dla.mil/Portals/104/Documents/Energy/Standard%20Prices/Aerospace%20Prices/E_2017Oct1AerospaceStandardPrices_170913.pdf?ver=2017-09-13-145335-477)
- [17] <https://www.mcmaster.com/aluminum/shape-round-tube/corrosion-resistant-3003-aluminum-tubes-7/>
- [18] <http://adb.moonsociety.org/04/03/09/01/dasa.html>

## Guidance and Navigation

- [1] [RL-ST16RT2-Data-Sheet.pdf \(rocketlabusa.com\)](#)
- [2] [D3408 CT2020 Updated 20211221.pdf \(ball.com\)](#)
- [3] [D1503 HAST 0118.pdf \(ball.com\)](#)
- [4] [arcsec Sagitta Star Tracker - CubeSatShop.com](#)
- [5] [PowerPoint-presentatie \(cubesatshop.com\)](#)
- [6] [2-pager- t3-star-tracker.pdf \(terma.com\)](#)
- [7] [STAR-T3 - Star Tracker | SatCatalog](#)
- [8] [NewSpace Sun Sensor 2020-10a \(cubesatshop.com\)](#)
- [9] [NSS Fine Sun Sensor - CubeSatShop.com](#)
- [10] [MIS21-011\\_Adcole\\_SpecSheets\\_Coarse\\_Sun\\_Sensor\\_R3\\_24\\_MAY\\_2021 \(1\).pdf](#)
- [11] [MIS21-001-Redwire-Brand-Fact-Sheet\\_MicroSunSensor\\_R4\\_28\\_APRIIL\\_2021.pdf](#)
- [12] [ISSTX Technical Specifications.pdf \(solar-mems.com\)](#)
- [13] [HG9900 Inertial Measurement Unit \(honeywell.com\)](#)
- [14] [LN-200S Inertial Measurement Unit \(IMU\) \(northropgrumman.com\)](#)
- [15] [EMCORE-EN-300-1-3-5-IMU.pdf](#)
- [16] [m-g370pdbs\\_briefsheet\\_e\\_rev20211001.pdf \(epson.com\)](#)
- [17] [HC7 and HC9 RWAs \(honeywell.com\)](#)
- [18] [NewSpace Reaction Wheel 20211018 \(newspacesystems.com\)](#)
- [19] [RL-RW-1.0-Data-Sheet.pdf \(rocketlabusa.com\)](#)
- [20] [Reaction Wheels - Vectronic Aerospace \(vectronic-aerospace.com\)](#)
- [21] [moog-integrated-avionics-unit-datasheet.pdf](#)
- [22] [SEAKR Catalog – Space off the Shelf](#)
- [23] [The Orion spacecraft is no smarter than your phone | Computerworld](#)
- [24] [SEAKR Catalog – Space off the Shelf](#)
- [25] [NIST Designs a Prototype Fuel Gauge for Orbit | NIST](#)
- [26] [On-Orbit Propellant Estimation, Management, and Conditioning for the THEMIS Spacecraft Constellation \(ucla.edu\)](#)

## Communications

- [1] [iris.pdf | SDL \(usu.edu\)](#)
- [2] [SatCatalog - Blue Canyon Technologies - BCT SDR - Datasheet.pdf](#)
- [3] [Working Copy TUI DATA SHEETS \(tethers.com\)](#)
- [4] [NANOCOM™ SOFTWARE DEFINED RADIO.pdf \(spacemicro.com\)](#)
- [5] [X-Band Patch Antenna - CubeSat Antenna | CubeSat by EnduroSat](#)
- [6] [syrlinks - X Band Patch Antenna for nano & cube satellites | Syrlinks](#)
- [7] [cavity-backed-spiral-antenna-800mhz-12ghz-ver1-21.pdf \(flexitech aerospace.com\)](#)
- [8] [cavity-backed-spiral-antenna-2-15ghz.pdf \(flexitech aerospace.com\)](#)
- [9] [DATASHEET \(isispace.nl\)](#)
- [10] [S-Band Patch Antenna CubeSat Module | CubeSat by EnduroSat](#)
- [11] [spaceborne-x-band-sspa-datasheet.ashx \(gdmissionsystems.com\)](#)
- [12] [41 dB Gain, 1 Watt Psat, 8 GHz to 12 GHz, Medium Power GaAs Amplifier, SMA Input, SMA Output, 3.5 dB NF Specifications \(pasternack.com\)](#)
- [13] [TGM2635-CP Data Sheet.pdf](#)
- [14] [Amplifiers - Solid State \(teledynedefenseelectronics.com\)](#)
- [15] [Spaceborne S-Band Solid State Power Amplifier - General Dynamics Mission Systems \(gdmissionsystems.com\)](#)
- [16] [47 dB Gain, 20 Watt P1dB, 3.1 GHz to 3.5 GHz, High Power Amplifier, SMA Input, SMA Output, 3.5 dB NF Specifications \(pasternack.com\)](#)
- [17] [Teledyne Paradise Datacom 500W S-Band Compact Outdoor GaN SSPA \(digisat.org\)](#)
- [18] [VSS3647 SSPA NF PG ONE 3-31-20 \(cpii.com\)](#)

## **Environmental**

- [1]<https://lunar.gsfc.nasa.gov/images/lithos/LROlitho7temperaturevariation27May2014.pdf>
- [2] SLS Mission Planner's Guide
- [3]<https://reader.elsevier.com/reader/sd/pii/S092145342030397X?token=9A5FCE51F754B199E50A08A156B357A644ECB0A7EA6DC5A2F573C800773445F775EBDD8A1E84573BE70DA5D4F3093118&originRegion=us-east-1&originCreation=20220427145954>
- [4][https://www.moog.com/content/dam/moog/literature/Space\\_Defense/spaceliterature/Vibration\\_Control/moog-shockwave-isolator-datasheet.pdf](https://www.moog.com/content/dam/moog/literature/Space_Defense/spaceliterature/Vibration_Control/moog-shockwave-isolator-datasheet.pdf)
- [5] [https://www.acousticalsurfaces.com/foam\\_stop/pdf/Flat-Faced\\_Melamine\\_Foam.pdf](https://www.acousticalsurfaces.com/foam_stop/pdf/Flat-Faced_Melamine_Foam.pdf)
- [6] <https://www-jstor-org.lp.hscl.ufl.edu/stable/44657664?seq=6>
- [7] <https://multimedia.3m.com/mws/media/1091998O/3m-fluorinert-electronic-liquids-for-heat-transfer-line-card.pdf>

## **Electrical**

- [1] [3.0 Power | NASA](#)
- [2] [BCT DataSheet Components PowerSystems.pdf \(bluecanyontech.com\)](#)
- [3] [redwire-roll-out-solar-array-flysheet \(1\).pdf](#)
- [4] [Power - ExoTerra Resource \(exoterracorp.com\)](#)
- [5] [Space Power Solutions - MMA Design LLC](#)
- [6] [SLC-21060-003 0322\\_0.pdf \(eaglepicher.com\)](#)
- [7] [GOMspace | NanoPower BP4](#)
- [8] [Standard Products | Ibeos](#)
- [9] [satsearch\\_17y2ic\\_vectronic\\_aerospace\\_gmb\\_h\\_li\\_ion\\_battery\\_block\\_vlb\\_4\\_8\\_16.pdf](#)
- [10] [AAC DataSheet Starbuck-Mini-updated.pdf \(aac-clyde.space\)](#)
- [11] [XPM2020 \(xes-inc.com\)](#)
- [12] [EPS II + Battery pack | CubeSat by EnduroSat](#)
- [13] [Products | Satellite Power Systems \(satellite-power-systems.de\)](#)

## Testing

[1] -chrome-  
extension://efaidnbmnnibpcajpcglclefindmkaj/viewer.html?pdfurl=https%3A%2F%2Fwww.nasa.gov%2Fcenters%2FJohnson%2Fpdf%2F639713main\_Vibration\_Testing\_FTI.pdf&clen=1049503&chunk=true

[2] -chrome-  
extension://efaidnbmnnibpcajpcglclefindmkaj/viewer.html?pdfurl=https%3A%2F%2Fwww.nasa.gov%2Fcenters%2FJohnson%2Fpdf%2F641784main\_Structures\_Test\_Lab\_FTI.pdf&clen=1177356&chunk=true

[3] -chrome-  
extension://efaidnbmnnibpcajpcglclefindmkaj/viewer.html?pdfurl=https%3A%2F%2Fwww.nasa.gov%2Fcenters%2FJohnson%2Fpdf%2F639724main\_Thermal\_Vacuum\_Testing\_FTI.pdf&clen=1274026&chunk=true

[4] -chrome-  
extension://efaidnbmnnibpcajpcglclefindmkaj/viewer.html?pdfurl=https%3A%2F%2Fwww.nasa.gov%2Fsites%2Fdefault%2Ffiles%2Fatoms%2Ffiles%2Fet10\_ptl.pdf&clen=1397489&chunk=true

[5] -https://www.intuitivemachines.com/post/moon-lander-engine-breaks-record-at-marshall-space-flight-center#:~:text=On%20February%202028%2C%202020%20Intuitive,firing%20of%20the%20same%20engine.

[6] -chrome-  
extension://efaidnbmnnibpcajpcglclefindmkaj/viewer.html?pdfurl=https%3A%2F%2Frs.nasa.gov%2Fapi%2Fcitations%2F20090032801%2Fdownloads%2F20090032801.pdf&clen=6791376

[7] -https://www.element.com/

## Appendices

### Appendix A: Open Items Status Report

Finalize electrical system design	Power calculations and circuit design	Electrical	Peak/typical power requirements have already been determined. Components have been selected
Finalize thermal system design	Power and heat transfer calculations	Environmental	Temperature ranges have already been determined along with a heat rejection system.
Further optimize structure	CAD Modeling and FEA	Mechanical	A complete model has been created for design review.
Begin Testing of all subsystems	Working with various firms for testing locations	Testing	Testing methods have been determined and roughly scheduled.
Calculating specific thrust values during takeoff and landing	Propulsion analysis, testing to find exhaust plume size	Propulsion/Flight Ops	Rough thrust amounts have been determined as part of operations to determine exhaust plume size.
Manufacture vehicle and parts	Following manufacturing schedule and creating physical parts	Mechanical	A schedule has been determined and vehicle structure has been determined. Part breakdowns are created and can be used for manufacturing.
Delivery and Delivery Prep	Ensure all systems are thoroughly tested, ensure all subsystems follow all required specifications.	Management	Plans for delivery date are in place and requirements from NASA have been studied to ensure they are met by delivery of vehicle.

## Appendix B: Trade Studies

### Structures

Criteria	Weight	Aluminum 7075-T6			Aluminum 7178-T6			Titanium 6A1-4V			M55J Carbon Fiber		
		Info	Value	Score	Info	Value	Score	Info	Value	Score	Info	Value	Score
Density [kg/m^3]	0.35	2810	6	2.1	2830	6	2.1	4430	3	30	1910	8	2.8
Yield Strength [MPa]	0.35	503	5	1.8	530	5	1.8	970	9	24	890	8	2.8
Material Cost [\$/kg]	0.15	5.2	9	1.4	3.3	9	1.4	21.2	3	80	15	6	0.9
Machinability [%]	0.15	70	7	1.1	70	7	1.1	20	2	20	0	1	0.2
				6.3			6.3			5.0			6.7

Figure 59: Material selection trade study.

## Mechanisms

Decision Criteria	Weight	ABL-024015P [10]			ABL-028010P [11]		
		Info	Value	Score	Info	Value	Score
Weight Kg	8	2.2	7	56	1.8	8	64
Capacity Ah	10	5	5	50	10	10	100
Energy Stored Wh	9	360	8	72	280	6	54
Cost \$	6	139.99	8	48	269.99	6	36
				226			254



Figure 60: PDM Battery Trade Study

Decision Criteria	Weight	KP5FN-22105-CVC [6]			Kawak Aviation BLDC [7]		
		Info	Value	Score	Info	Value	Score
Weight Kg	8	0.303	10	80	11.8	4	32
Power/Volt/Cur	5	13W/28Vdc/0.7A	5	25	4kW/28Vdc/140A	8	40
Cost \$	7	40.5	10	70	500	5	35
Torque Nm	6	0.0235	5	30	11.8	8	48
RPM	6	5200	7	42	3150	5	30
				247			185



Figure 61: PDM Deployment Motor Trade Study

Decision Criteria	Weight	6627T103 [8]			6627T102 [9]		
		Info	Value	Score	Info	Value	Score
Weight Kg	8	0.998	8	64	0.68	9	72
Power/Volt/Cur	5	12-40vDc/0.3-3A	10	50	12-40vDc/0.3-3A	10	50
Cost \$	7	684.4	6	42	676.73	7	49
Hold torque Nm	9	2.08	9	81	1.29	6	54
RPM	4	750	5	20	2160	7	28
				257			253



Figure 62: PDM Locking Motor Trade Study

		Deployable Landing Gear (PTK NP)[1][2]			Stationary Landing Gear		
Decision Criteria	Weight	Info	Value	Score	Info	Value	Score
Storage Space	8	Limited by SLT	10	80	Limited by legs	5	40
Cost	6	More expensive due to complexity	3	18	Less expensive and easy to manufacture	7	42
Simplicity	7	More moving parts and electronics	3	21	No moving parts or extra hardware/software	10	70
TRL	9	9	10	90	8	8	72
				209			224



Figure 63: Landing Legs Trade Study

		Crush Honeycomb & Hydraulic Damping [3][4]			Only Hydraulic damping [5][14]			Metal Bellows damping [12]			Electromagnetic Shock Absorber [13]		
Decision Criteria	Weight	Info	Value	Score	Info	Value	Score	Info	Value	Score	Info	Value	Score
Damping	8	System will be tuned to the SLT to provide a soft landing	5	40	System will be tuned to the SLT to provide a soft landing	5	40	System will be tuned to the SLT to provide a soft landing	5	40	System will be tuned to the SLT to provide a soft landing	5	40
Cost	6	No exact cost provided	8	48	No exact cost provided but is more expensive due to reliability	6	36	No exact cost provided but is less expensive the space grade hydraulics but more expensive than crush honeycomb	7	42	No exact cost provided but is the most expensive due to complexity	4	24
Reusability	10	One time use	1	10	Reusable	10	100	Reusable	10	100	Reusable	10	100
TRL	9	9	9	81	8	8	72	7	8	72	7	8	72
Reliability	10	Best	10	100	Good	6	60	Great	8	80	Good	6	60
			279			308			334			296	



Figure 64: Shock Absorber Trade Study

## Propulsion

Criteria	Weight	N <sub>2</sub> H <sub>4</sub> + Catalyst			MMH/NTO			LCH <sub>4</sub> /LOX			LH <sub>2</sub> /LOX		
		Mag.	Value	Score	Info	Value	Score	Info	Value	Score	Info	Value	Score
Bulk Density [g/cm <sup>3</sup> ]	10	1.01	8.4	84.2	1.20	10.0	100.0	0.83	6.9	69.2	0.32	2.7	26.7
Heritage	8	10	10.0	80.0	10	10.0	80.0	0	0.0	0.0	5	5.0	40.0
Thermal Sensitivity	-4	0	0.0	0.0	2	2.0	-8.0	6	6.0	-24.0	10	10.0	-40.0
Corrosivity	-2	2	2.0	-4.0	10	10.0	-20.0	0	0.0	0.0	0	0.0	0.0
Char. Velocity [m/s]	8	1333	5.6	44.7	1724	7.2	57.8	1838	7.7	61.6	2386	10.0	80.0
				<b>204.9</b>			<b>209.8</b>			<b>106.8</b>			<b>106.7</b>

Figure 65: Propellant type trade study.

		R-40 (AJRD), 4x			S3K (DASA/EADS), 4x			Aestus (ArianeGroup)		
Criteria	Weight	Mag.	Value	Score	Info	Value	Score	Info	Value	Score
Thrust [kN]	4	16.0	5.4	21.6	14.0	4.7	18.9	29.6	10.0	40.0
Isp [s]	10	293	8.3	83.2	352	10.0	100.0	324	9.2	92.0
Controllability	6	10	10.0	60.0	10	10.0	60.0	5	5.0	30.0
Size Factor [kg <sup>-1</sup> ]	2	0.037	10.0	20.0	0.017	4.7	9.4	0.009	2.5	4.9
				<b>264.9</b>			<b>268.3</b>			<b>246.9</b>

Figure 66: Main engine trade study.

## Guidance and Navigation

		ST-16RT2 [1]			HAST [2,3]			Sagitta [4,5]			T3 [6,7]		
Criteria	Weight	Info	Value	Score	Info	Value	Score	Info	Value	Score	Info	Value	Score
Mass [g]	10	158	10	100	9000	1	10	275	10	100	350	10	100
Accuracy [arcsec]	5	5	5	25	0.18	9	45	2	7	35	0.1	10	50
Price [K USD]	7	120	7	49	750	3	21	50	10	70	83	9	63
Power [W]	8	1	10	80	12	1	8	1.4	10	80	2	8	64
				254			84			285			277

Figure 67: Star tracker trade study.

		NFSS-411 [8,9]			Coarse Cosine [10]			RedwireMicro [11]			ISST60 [12]		
Criteria	Weight	Info	Value	Score	Info	Value	Score	Info	Value	Score	Info	Value	Score
Mass [g]	10	35	6	60	10	8	80	2	10	100	100	1	10
Accuracy [ $^{\circ}$ RMS]	6	0.1	8	48	5	4	24	5	4	24	0.06	10	60
Price [K USD]	7	12	10	70	20	5	35	20	5	35	20	5	35
Power [W]	5	0.15	8	40	0	10	50	0	10	50	1	9	45
				218			189			209			150

Figure 68: Sun sensor trade study.

		HG9900 [13]			LN-200S [14]			EN-300 [15]			M-G370PDS0 [16]		
Criteria	Weight	Info	Value	Score	Info	Value	Score	Info	Value	Score	Info	Value	Score
Mass [g]	10	2700	1	10	748	4	40	800	4	40	10	10	100
Accuracy [ $^{\circ}/hr$ ]	7	0.0035	10	70	1	5	35	0.1	7	49	0.8	6	63
Accuracy [ $\mu g$ ]	7	25	9	63	300	5	35	300	5	35	12	10	70
Power [W]	5	10	7	50	12	6	30	18	5	25	0.05	10	50
				193			140			149			283

Figure 69: IMU trade study.

		HC9 [17]			NRWA-T6 [18]			RW-1.0 [19]			VRW-D-6 [20]		
Criteria	Weight	Info	Value	Score	Info	Value	Score	Info	Value	Score	Info	Value	Score
Mass [g]	10	5500	5	50	4600	6	60	1380	10	100	3000	8	80
Momentum [Nms]	9	11.5	10	90	5.45	6	54	1.0	3	21	6	6	54
Torque [Nm]	9	0.2	10	90	0.110	7	63	0.1	7	63	0.09	5	45
Power [W]	5	130	5	25	130	5	25	43	10	50	110	5	25
				255			202			234			204

Figure 70: Reaction wheel trade study

		Moog IAU [21]			Seakr C&DH [22]			Orion [23]			Athena-3 [24]		
Criteria	Weight	Info	Value	Score	Info	Value	Score	Info	Value	Score	Info	Value	Score
Mass [g]	10	8300	5	50	5300	6	60	2000	9	90	1000	10	100
TRL	8	9	10	80	8	8	64	5	5	40	9	10	80
Power [W]	6	37	7	42	14	10	60	50	6	36	16	9	54
				172			184			166			234

Figure 71: Flight computer trade study.

		ECTV [25]			Bookkeeping [26]			Thermal Gauging [26]			PVT [26]		
Criteria	Weight	Info	Value	Score	Info	Value	Score	Info	Value	Score	Info	Value	Score
TRL	8	3	6	48	9	9	72	9	9	72	9	9	72
Simplicity	10	7	7	70	10	10	100	5	5	50	7	7	70
Accuracy Trend	6	none	10	60	increases	5	30	decreases	9	54	increases	5	30
				178			202			176			172

Figure 72: Fuel estimation trade study.

### Communications

		IRIS [1]			BCT-SDR [2]			Swift-XTS [3]			Nanocom [4]		
Criteria	Weight	Info	Value	Score	Info	Value	Score	Info	Value	Score	Info	Value	Score
Mass [kg]	10	1.1	6	60	0.25	10	100	0.8	8	80	1.5	5	50
Bands	5	X,Ka,S	10	50	X,Ka,S	10	50	X,S	6	30	X,Ka,S	10	50
Data Rate [Mbps]	7	1	1	7	100	8	56	25	3	21	300	10	70
Power [W]	8	35	7	56	34	8	64	22	10	80	35	7	56
				193			270			211			226

Figure 73: SDR trade study.

		EnduroSat[5]			Span-X-T2 [5]			800MHz - 12GHz [7]			2-15GHz [8]		
Criteria	Weight	Info	Value	Score	Info	Value	Score	Info	Value	Score	Info	Value	Score
Mass [g]	10	2.2	10	100	68	8	80	714	4	40	173	7	70
Gain [dBi]	6	6	9	54	7.6	10	60	3	7	42	3	7	42
Bands	8	X	5	40	X	5	40	X,S	10	80	X,S	10	80
Power [W]	5	4	10	50	NL	5	25	10	6	30	10	6	30
				244			205			192			222

Figure 74: X-band antenna trade study.

		ISISpace [9]			EnduroSat[10]			800MHz - 12GHz [7]			2-15GHz [8]		
Criteria	Weight	Info	Value	Score	Info	Value	Score	Info	Value	Score	Info	Value	Score
Mass [g]	10	50	10	100	64	9	90	714	3	30	173	7	70
Gain [dBi]	6	6.5	8	48	8.3	10	60	3	4	24	3	4	24
Bands	8	S	5	40	S	5	40	X,S	10	80	X,S	10	80
Power [W]	5	2	10	50	4	8	40	10	4	20	10	4	20
				238			230			154			194

Figure 75: S-band antenna trade study.

		General Dynamics [11]			PE15A4008 [12]			TGM 2635-CP [13]			Teledyne [14]		
Criteria	Weight	Info	Value	Score	Info	Value	Score	Info	Value	Score	Info	Value	Score
Mass [g]	10	1370	1	10	16.37	9	90	15	10	100	360	4	40
Output [W]	6	17	2	12	1	1	6	100	10	60	25	3	18
Range [GHz]	8	7.8 to 8.8	3	24	8 to 12	10	80	7.9 to 11	7	56	7 to 8	3	24
Power [W]	5	65.5	5	25	14.4	9	45	5	10	50	100	1	5
			71				221			266			87

Figure 76: X-band amplifier trade study.

		General Dynamics [15]			PE15A5003 [16]			Teledyne [17]			VSS3647 [18]		
Criteria	Weight	Info	Value	Score	Info	Value	Score	Info	Value	Score	Info	Value	Score
Mass [g]	10	1980	3	30	5.72	10	100	20	8	80	6350	1	10
Output Power [W]	6	8.3	4	24	20	5	30	500	6	36	1500	10	60
Range [GHz]	8	2.2 to 2.3	1	8	3.1 to 3.5	4	32	1.75 to 2.3	6	48	3.1 to 3.5	4	32
Power [W]	5	37	10	50	108	8	40	250	6	30	450	4	20
			112				202			194			122

Figure 77: S-band antenna trade study.

## Environmental

		Aluminum 6063 w/ 10 mil silver teflon			Aluminum w/ 5mil Silver Teflon Coating			Aluminum Teflon Coat 5 mil		
Selection Criteria	Weight	Magnitude	Score	Value	Magnitude	Score	Value	Magnitude	Score	Value
Heat Flux per Change in Kelvin (W/K-m^2)	10	1749.84	6	60	3151.27	10	100	3149.60	9	90
Cost [\$/cm^2]	5	0.11	3	15	0.058	6	30	0.0046	10	50
Absorption (EOL)	7	0.09	9	63	0.08	10	70	0.23	5	35
Density (g/cm^2)	9	3.60	7	63	3.51	9	81	3.49	10	90
Emmisivity	8	0.85	10	80	0.78	8	64	0.75	7	56
					281			345		321

Figure 78: Radiator material selection [6].

		Fluoronert FC-40			Liquid Ammonia		
Selection Criteria	Weight	Magnitude	Score	Value	Magnitude	Score	Value
Heat Dissipation (W/m-K)	8	0.07	10	80	0.03	5	40
Cost [\$/kg]	5	295	2	10	0.88	10	50
Boiling Point	10	155 at 1atm	9	90	100 C at >75atm	6	60
				180			150

Figure 79: Thermal fluid selection [7].

		Moog Shockwave			Sorbothane Anti-vibration and Leveling		
Selection Criteria	Weight	Magnitude	Score	Value	Magnitude	Score	Value
Diameter [cm]	7	4.67	10	70	8.89	8	56
Mass [kg]	10	0.08	10	100	0.113	9	90
Stiffness [lbf/in]	6	2300	8	48	820-2000	8	48
				218			194

Figure 80: Vibration damper selection.

		Flat Face Melamine Foam 1"			Flat Face Melamine Foam 2"			Ester Type Acoustic Foam 1"			Ester Type Acoustic Foam 2"		
Criteria	Weight	Mag.	Score	Value	Mag.	Score	Value	Mag.	Score	Value	Mag.	Score	Value
Density [kg/m <sup>3</sup> ]	10	8.97	10	100	8.97	10	100	32.04	5	50	32.04	5	50
Absorption at 1kHz	7	0.7	6	42	1.25	9	63	0.55	5	35	1.13	8	56
Absorption at 2kHz	7	0.8	6	42	1.15	9	63	0.85	7	49	0.92	8	56
Cost [\$/m <sup>2</sup> ]	5	140	10	50	280	7	35	160	9	45	320	6	30
				234			261			179			192

Figure 81: Acoustic foam selection.

## Electrical

		Solar [1]			Nuclear [1]			Fuel Cell [1]			
Criteria		Weight	Info	Value	Score	Info	Value	Score	Info	Value	Score
Power Output [kW]	8	11	10	80	0.3	4	32	10	9	72	
Typical Mass [kg]	10	1	10	100	50	5	50	30	6	60	
Efficiency [%]	6	30	9	54	6	6	36	40	10	60	
Refuel Frequency	5	Daily	5	25	Decades	7	35	Rarely	10	50	
				259			153			242	

		BCT [2]				ROSA [3]				FOSA [4]				rHAWK [5]		
Criteria	Weight	Info	Value	Score	Info	Value	Score	Info	Value	Score	Info	Value	Score	Info	Value	Score
Power Provided [W]	10	400	5	50	30,000	10	100	300	4	40	6000	7	70			
Specific Power [W/kg]	8	90	5	40	120	8	64	140	10	80	130	9	72			
Deployment	5	Release Mechanism	5	25	Strain Energy	10	50	Release Mechanism	5	25	Boom Deployed	7	35			
			115			214			145			177				

		SLC-2 1060-003 [6]			NanopowerBP4 [7]			Ibeos [8]			VLB-X [9]		
Criteria	Weight	Info	Value	Score	Info	Value	Score	Info	Value	Score	Info	Value	Score
Mass [g]	10	1974	4	40	258	10	100	1000	5	50	4500	2	20
Energy Density [Wh/L]	7	324.1	10	70	211.9	7	49	151.1	6	42	74.6	5	35
Specific Energy [Whr/kg]	7	131.7	9	63	149.2	10	70	109.8	7	49	101.96	6	42
Capacity [Ah]	8	72	10	80	5.2	3	24	10	5	40	12	6	48
				253			243			181			145

		Starbuck-Mini [10]			X PM2020 [11]			EPS II [12]			PCU-SB7 [13]		
Criteria	Weight	Info	Value	Score	Info	Value	Score	Info	Value	Score	Info	Value	Score
Mass [kg]	9	3.3	6	54	0.66	10	90	1.28	8	72	1.5	7	63
System Power [W]	10	1500	10	100	300	5	50	250	4	40	250	4	40
Power Consumption [W]	8	10	7	56	5	10	80	10	7	56	10	7	56
Efficiency [%]	5	90	10	50	85	7	35	86	8	40	85	7	35
				260			255			208			194

## Appendix C: Calculations

### Structures

#### Landing Legs

##### Mesh information

Mesh type	Mixed Mesh
Mesher Used:	Standard mesh
Automatic Transition:	Off
Include Mesh Auto Loops:	Off
Jacobian points for High quality mesh	16 Points
Jacobian check for shell	On
Element Size	5.31635 mm
Tolerance	0.265817 mm
Mesh Quality	High

##### Beams

###### Beam Forces

Beam Name	Joint s	Axial(N )	Shear1(N )	Shear2(N )	Moment1(N.m )	Moment2(N.m )	Torque(N.m )
Beam-1(Al round tubing AL RND TUBE 2.5 OD X 0.25 WALL(3))	1	-3,862.46	39.5671	-39.4465	42.4942	41.6636	28.6167
	2	3,862.46	-39.5687	39.4473	2.34065	3.30556	-28.6167
Beam-2(Al round tubing AL RND TUBE 2.5 OD X 0.25 WALL(2))	1	-7,545.36	-3,125.31	0.00243985	3.32532e-06	-171.896	1.35164e-06
	2	7,545.34	3,125.35	0.00243985	0.00206084	2,816	-1.35161e-06
Beam-3(Al round tubing AL RND TUBE 3.5 OD X 0.5 WALL(1))	1	10,469.6	-1,351.68	0.00741966	0.0946115	-18.7398	-0.14489
	2	-7,545.34	-3,125.36	0.00243985	-0.00206084	-2,816	1.35523e-06
Beam-4(Mirror14[4])	1	-3,862.39	-39.5391	-39.2697	42.5894	-41.5931	-28.4547
	2	3,862.4	39.5329	39.2672	2.04356	-3.33875	28.4547

###### Beam Stresses

Beam Name	Joints	Axial(N/m^2)	Bending Dir1(N/m^2)	Bending Dir2(N/m^2)	Torsional (N/m^2)	Upper bound axial and bending(N/m^2)
Beam-1(Al round tubing AL RND TUBE 2.5 OD X 0.25 WALL(3))	1	3.38785e+06	-2.86327e+06	2.8073e+06	964,101	7.39774e+06
	2	3.38785e+06	157,713	-222,730	-964,100	3.66076e+06
Beam-2(Al round tubing AL RND TUBE 2.5 OD X 0.25 WALL(2))	1	-6.6182e+06	0.224061	1.15824e+07	0.0455369	1.82006e+07
	2	-6.61819e+06	-138.86	1.89743e+08	-0.0455358	1.96361e+08
Beam-3(Al round tubing AL RND TUBE 3.5 OD X 0.5 WALL(1))	1	-3.44368e+06	-1,854.33	-367,289	-1,419.88	3.81098e+06
	2	-2.48182e+06	-40.3913	5.5192e+07	0.0132809	5.76739e+07
Beam-4(Mirror14[4])	1	3.38779e+06	-2.86968e+06	-2.80255e+06	-958,643	7.39895e+06
	2	3.38779e+06	137,696	224,966	958,641	3.65155e+06

## Engine Mounts

### Study Properties

<b>Study name</b>	Static 1
<b>Analysis type</b>	Static
<b>Mesh type</b>	Mixed Mesh
<b>Thermal Effect:</b>	On
<b>Thermal option</b>	Include temperature loads
<b>Zero strain temperature</b>	298 Kelvin
<b>Include fluid pressure effects from SOLIDWORKS Flow Simulation</b>	Off
<b>Solver type</b>	Automatic
<b>Inplane Effect:</b>	Off
<b>Soft Spring:</b>	Off
<b>Inertial Relief:</b>	Off
<b>Incompatible bonding options</b>	Automatic
<b>Large displacement</b>	Off
<b>Compute free body forces</b>	On
<b>Friction</b>	Off
<b>Use Adaptive Method:</b>	Off
<b>Result folder</b>	SOLIDWORKS document (C:\Users\admin\Documents\CDR\CAD)

### Mesh information

<b>Mesh type</b>	Mixed Mesh
<b>Mesher Used:</b>	Curvature-based mesh
<b>Jacobian points for High quality mesh</b>	16 Points
<b>Jacobian check for shell</b>	On
<b>Maximum element size</b>	122.042 mm
<b>Minimum element size</b>	24.4085 mm
<b>Mesh Quality</b>	High

### Mesh information - Details

<b>Total Nodes</b>	34162
<b>Total Elements</b>	16557
<b>Time to complete mesh(hh:mm:ss):</b>	00:00:11
<b>Computer name:</b>	

## Resultant Forces

### Reaction forces

Selection set	Units	Sum X	Sum Y	Sum Z	Resultant
Entire Model	N	-0.00500843	-86,000	0.00517219	86,000

### Reaction Moments

Selection set	Units	Sum X	Sum Y	Sum Z	Resultant
Entire Model	N.m	0	0	0	1e-33

### Free body forces

Selection set	Units	Sum X	Sum Y	Sum Z	Resultant
Entire Model	N	0.0039978	-0.0250854	0.024704	0.0354337

### Free body moments

Selection set	Units	Sum X	Sum Y	Sum Z	Resultant
Entire Model	N.m	-0.695185	-1.41882e-07	-0.249718	0.738676

## Beam Forces

Beam Name	Joint s	Axial(N )	Shear1(N )	Shear2(N )	Moment1(N.m)	Moment2(N.m)	Torque(N.m )
Beam-2(Body-Move/Copy9[5])	1	61.6831	13.4401	104.673	-30.0018	3.64029	16.816
	2	61.6831	-13.4401	-104.673	-29.0108	3.93702	-16.816
Beam-26(Body-Move/Copy9[3])	1	36.7595	-17.3201	-78.9147	25.4397	-4.39319	10.7921
	2	36.7595	17.3201	78.9147	19.0509	-5.37156	-10.7921
Beam-41(Mirror5[3])	1	159.263	1,068.03	-39.292	21.7488	367.591	21.2199
	2	159.263	-1,068.03	39.292	0.4033	234.545	-21.2199
Beam-42(Al tube square AL TUBE 1.5 SQR X 0.095 WALL(2)[7])	1	58.5702	-1,002.82	-15.3273	1.09864	-224.643	20.8355
	2	58.5702	1,002.82	15.3273	7.5426	-340.729	-20.8355
Beam-43(Al tube square AL TUBE 1.5 SQR X 0.095 WALL(2)[5])	1	72.3359	152.205	-22.2782	3.02881	40.2634	-2.73143
	2	72.3359	-152.205	22.2782	9.53122	45.5469	2.73143

## Beam Stresses

Beam Name	Joints	Axial(N/m^2)	Bending Dir1(N/m^2)	Bending Dir2(N/m^2)	Torsional (N/m^2)	Upper bound axial and bending(N/m^2)
Beam-2(Body-Move/Copy9[5])	1	179,077	7.78152e+06	944,178	3.99736e+06	8.90478e+06
	2	179,077	-7.5245e+06	-1.02114e+06	3.99736e+06	8.72472e+06
Beam-26(Body-Move/Copy9[3])	1	106,719	-6.59827e+06	-1.13946e+06	2.56541e+06	7.84445e+06
	2	106,719	4.94122e+06	1.39322e+06	2.56541e+06	6.44116e+06
Beam-41(Mirror5[3])	1	462,367	-5.64097e+06	9.53417e+07	5.04407e+06	1.01445e+08
	2	462,367	104,604	-6.08338e+07	5.04407e+06	6.14008e+07
Beam-42(Al tube square AL TUBE 1.5 SQR X 0.095 WALL(2)[7])	1	-170,039	-284,953	-5.82653e+07	4.95285e+06	5.87203e+07
	2	-170,039	1.95631e+06	8.83745e+07	4.95285e+06	9.05009e+07
Beam-43(Al tube square AL TUBE 1.5 SQR X 0.095 WALL(2)[5])	1	210,004	-785,578	1.04431e+07	-649,295	1.14386e+07
	2	210,004	2.4721e+06	-1.18134e+07	649,295	1.44956e+07

## Propulsion

ENGINE DATA					
Engine Type DASA S3K	Thrust (N) 3500	Dry Mass (kg) 14.5	Isp (s)	P_chamber (atm) 352	# of Engines 9

VEHICLE MASS DATA (kg)					
<i>Payload</i>	Max. payload mass (kg) 200				
<i>Bus</i>	ACS/Comms 116.031	Power 10	Mechanisms 25	Structure 342	
<i>Propulsion</i>	Thrusters 63.12	Valves/pipes 10	Tanks 84.7	Propellant 1337.17	
<i>Total</i> (kg) (N, surf.)	Bus Only 493.031 801.04	Bus + Payload 693.031 1125.98	Dry 850.851 1382.39	Wet 2188.021 3554.92	

ENVIRONMENT DATA					
grav. param. ( $m^3/s^2$ ) 4.90E+12	radius (m) 1.74E+06	lun. grav. ( $m/s^2$ ) 1.62E+00	std. grav. ( $m/s^2$ ) 9.80665		

FUEL DATA					
Fuel Type MMH	Oxidizer Type MON-3	Mixture Ratio 2.1	Cycle Type pressure-fed		
<i>Pressurant</i> Helium	Tank Mass (kg) 12.7	Tank Vol. ( $m^3$ ) 0.0814	Pres. Mass (kg) 4.48	M.M. (kg/mol) 4.00E-03	
MEOP (bar) 331		Tank Vol. (L) 81.4			
Pressure (bar) 300	Pressure (atm) 296.0769	Temp (C) 0	Temp (K) 273.15	# Tanks 1	
<i>Fuel</i>	Tank Mass (kg) 36	Tank Vol. ( $m^3$ ) 0.7	Fuel Mass (kg) 429.9	M.M. (kg/mol) 4.61E-02	
MEOP (bar) 22		Tank Vol. (L) 700		Density ( $kg/m^3$ ) 870	
Pressure (bar) 16.4	Pressure (atm) 16.1855372	Temp (C) 0	Temp (K) 273.15	# Tanks 1	
<i>Oxidizer</i>	Tank Mass (kg) 36	Tank Vol. ( $m^3$ ) 0.7	Ox. Mass (kg) 902.79	M.M. (kg/mol)	
MEOP (bar) 22		Tank Vol. (L) 700	PROP LOAD (%) 90	Density ( $kg/m^3$ ) 1433	
Pressure (bar) 16.4	Pressure (atm) 16.1855372	Temp (C) 0	Temp (K) 273.15	# Tanks 1	

VELOCITY DATA (m/s)					
NRHO->LLO 750	LLO->surf 2000	hop 1 2067.87	hop 2 2067.87	round-trip 4135.74	

THRUST DATA			
Comb. Thrust (N)	TWR, min.	accel. (m/s^2)	
14000	3.938208548	6.398476066	

<b>HOP FLIGHT CALCULATIONS</b>		<i>hover angle theta (deg):</i>		14.71
		<i>(rad):</i>		0.2567
Parabolic bullet trajectory:	Range (km)	Launch angle (d)	(rad)	V_i (m/s)
	301.5909052	45	0.785398163	700
	V_x	V_y	t_f (s)	h_max (m)
	494.9747468	494.9747468	609.31	75397.73
			dV	700
Rectangular flight traj.:	BURN I	burn time (s)	Vy_1 (m/s)	t_c (s)
min. hover = 7010m		90.0	429.6382773	264.44
		y_b (m)	y_c (m)	hover height (m)
		19333.72	56806.51	76140.23
t+	BURN 2	burn time (s)	Vx_2 (m/s)	coast time (s)
354.44		94.0	581.74	247.0
		x_b (m)	coast range (m)	LB1 height (m)
		27341.96	143690.70	26579.04
			burn angle (deg)	dV
t+	LB1		47.0	601.46
695.44		131.37		0.82
		Vxi (m/s)	x_f (m)	
impact time from LB1 (free):		581.74	-401.31	131209.47
59.15		Vxf (m/s)	Vyf (m/s)	y_f (m)
				dV
		8.49	0.00	840.55096
				26
t+	LB2	Estimated. Based on terrain.		
826.81				dV
				50
	Total Time (s):	826.806		
	Total Range (km):	302.2421234	Total Hop dV:	2067.87

## Guidance and Navigation

### Mass Calculations

#### **Typical Flight**

Star Trackers: 3(275 g) = 825 g

Sun Sensors: 8(35 g) = 280 g

IMU: 2(10 g) = 20 g

Reaction Wheels: 4(5500 g) = 22000 g

Flight Computer: 2(1000 g) = 2000 g

Total: 25,125 g = 25.125 kg

#### **Descent and Landing**

Cameras: 10(0.425 kg) = 4.25 kg

Altimeter: 2(10 kg) = 20 kg

IMU: 1(0.010 kg) = 0.010 kg

HDL: 1(30 kg) = 30 kg

NDL: 1(30 kg) = 30 kg

Descent and Landing Computer: 1(6 kg) = 6 kg

Total: 90.26 kg

### Cost Calculations

#### **Typical Flight**

Star Trackers: 3(\$50K) = \$150K

Sun Sensors: 8(\$12K) = \$96K

IMU: 2(\$10K) = \$20K

Reaction Wheels: 4(\$15K) = \$60K

Flight Computer: 2(\$200K) = \$400K

Total: \$726K

### Power Calculations

#### **Typical Flight**

Star Trackers: 2(1.4 W) = 2.8 W

Sun Sensors: 4(0.15 W) = 0.6 W

IMU: 1(0.05 W) = 0.05 W

Reaction Wheels: 3(130 W) = 390 W

Flight Computer: 1(16 W) = 16 W

Total: 409.45 W

#### **Descent and Landing**

Cameras: 7(5 W) = 35 W

Altimeter: 1(10 W) = 10 W

IMU: 1(0.05 W) = 0.05 W

HDL: 1(85 W) = 85 W

NDL: 1(85 W) = 85 W

Descent and Landing Computer: 1(50 W) = 50 W

Total: 265.05 W

## Communications

### **Mass Calculations**

SDR:  $2(250 \text{ g}) = 500 \text{ g}$

X-band Antenna:  $2(2.2 \text{ g}) = 4.4 \text{ g}$

S-band Antenna:  $2(50 \text{ g}) = 100 \text{ g}$

X-band Amplifier:  $2(15 \text{ g}) = 30 \text{ g}$

S-band Amplifier:  $2(5.72 \text{ g}) = 11.44 \text{ g}$

Total:  $645.84 \text{ g} = 0.646 \text{ kg}$

### **Power Calculations**

SDR:  $1(34 \text{ W}) = 34 \text{ W}$

X-band Antenna:  $1(4 \text{ W}) = 4 \text{ W}$

S-band Antenna:  $1(2 \text{ W}) = 2 \text{ W}$

X-band Amplifier:  $1(5 \text{ W}) = 5 \text{ W}$

S-band Amplifier:  $1(5 \text{ W}) = 5 \text{ W}$

Total:  $50 \text{ W}$

### **Cost Calculations**

SDR:  $2(\$30K) = \$60K$

X-band Antenna:  $2(\$4.5K) = \$9K$

S-band Antenna:  $2(\$4.5K) = \$9K$

X-band Amplifier:  $2(\$2.2K) = \$4.4K$

S-band Amplifier:  $2(\$5K) = \$10K$

Total:  $\$92.4K$

## **Environmental**

### MLI Layers:

- Aluminized Beta Cloth
- Dacron Netting Spacer Layer
- Aluminized Kapton

The netting and Kapton are repeated such that there are 8 reflective layers and 9 netting layers. This results in a total mass of  $0.18 \text{ g/cm}^3$  and a total absorption of 0.135.

As for solar radiation, the sun radiates  $1360 \text{ W/m}^2$ . Estimating our craft as a 4 meter diameter sphere, the craft should absorb 5440 W of solar radiation. Using the 18-layer MLI, this is reduced to 735 W.

## Appendix D: Requirements Matrices

Standard	Description	Status	Comments
ASD-SLT-01	The SLT shall be capable of launching as a Co-manifested Payloads (CPL) on the Space Launch System (SLS). The SLT should also be compatible with a suitable commercial launch vehicle.	Complete	
ASD-SLT-02	The SLT shall be qualified for structural loads per ESD 30000 Mission Planner's Guide. The SLT should also be compatible with a suitable commercial launch vehicle.	Complete	
ASD-SLT-03	The SLT shall be qualified for shock loads per ESD 30000 Mission Planner's Guide. The SLT should also be compatible with a suitable commercial launch vehicle.	Complete	
ASD-SLT-04	The SLT shall be qualified for Acoustic Loads per ESD 30000 Mission Planner's Guide. The SLT should also be compatible with a suitable commercial launch vehicle.	Complete	
ASD-SLT-05	The SLT shall be qualified for Vibration Loads per ESD 30000 Mission Planner's Guide. The SLT should also be compatible with a suitable commercial launch vehicle.	Complete	
ASD-SLT-06	The SLT shall be qualified for Thermal Loads per ESD 30000 Mission Planner's Guide. The SLT should also be compatible with a suitable commercial launch vehicle.	Complete	
ASD-SLT-07	The SLT shall be qualified for pre-launch purge and ascent venting profiles per ESD 30000 Mission Planner's Guide. The SLT should also be compatible with a suitable commercial launch vehicle.	Complete	
ASD-SLT-08	The SLT shall be compatible with electrical bonding and grounding requirements per ESD 30000 Mission Planner's Guide. The SLT should also be suitable compatible with a commercial launch vehicle.	Complete	
ASD-SLT-09	The SLT shall have a total mass at launch of not more than 2,000 Kg not including launch vehicle attach hardware.	Complete	
ASD-SLT-010	The SLT shall have a spacecraft coordinate system compliant with ESD 30000 Mission Planner's Guide. The SLT should also be compatible with a suitable commercial launch vehicle.	Complete	
ASD-SLT-011	SLT Center of Gravity (CG) shall be calculated and documented and in compliance with ESD 30000 Mission Planner's Guide. The SLT should also be compatible with a suitable	Complete	
ASD-SLT-012	The SLT shall not generate debris as a consequence of normal operation.	Complete	
ASD-SLT-013	The SLT shall minimize the lunar regolith ejected when launching from or landing on unimproved landing sites.	Complete	
ASD-SLT-014	The Moments and Products of Inertia shall be calculated in both the pre- and post deployment configuration of the SLT. Pre-deployment is defined as the SLT configuration when stowed for launch. Post-deployment is defined as the SLT configuration while in its mission mode.	Complete	
ASD-SLT-015	The SLT shall have a payload capacity of 200Kg mass.	Complete	Complete

ASD-SLT-016	The SLT shall be capable of accommodating a payload having a volume of 1.2m long by 0.5m tall by 0.5m wide.	Complete	
ASD-SLT-017	The SLT shall define a standard payload mechanical, electrical and communication interface for all suitable payloads. The interfaces should conform to industry standards established for CubeSat interfaces with launch vehicle providers.	Complete	
ASD-SLT-018	The SLT shall be capable of providing 28V DC power to payloads for the duration of the mission	Complete	
ASD-SLT-019	The SLT shall be capable of accommodating a payload requiring to communicate to surface or space based operators via X-band radio.	Complete	
ASD-SLT-020	The SLT shall have a payload capacity of carrying a 200Kg mass payload to a maximum operational limit of 300Km and return that mass to the point of origin in one operational cycle without the need for refueling or refurbishment.	Complete	
ASD-SLT-021	The SLT shall provide a fuel capacity that would support performing a minimum of 1.1 round-trips to the maximum operational limit without refueling. The SLT <b>may</b> either be capable of delivering itself from lunar orbit or be delivered aboard a Commercial Lunar Payload Service lander.	Complete	
ASD-SLT-022	The SLT shall support full flight and payload support capabilities during Lunar day conditions and up to 72 hours in Lunar night conditions.	Complete	
ASD-SLT-023	The SLT <b>should</b> support limited operational capabilities including, but not limited to communication and temperature maintenance for a period no less than ½ of a Lunar night cycle.	Complete	
ASD-SLT-024	The SLT shall have the ability to launch after landing within 20 minutes without refueling within one mission cycle.	Complete	
ASD-SLT-025	The SLT shall be able to navigate to and land at a designated location with a precision of 10 meter. Terminal guidance shall allow for hazardous terrain avoidance at unimproved landing sites. Navigation may utilize inertial guidance and homing beacons depending on mission needs.	Complete	
ASD-SLT-026	The SLT shall be able to transmit and receive data and commands with SCS and remote sites either by line of sight or via relay satellite/tower as appropriate for the situation utilizing X-band radio.	Complete	
ASD-SLT-027	A plan shall be developed for SLT end to end testing utilizing guidelines found in the compliance documents section.	Complete	
ASD-SLT-028	A graphic shall be created which represents the purpose of the mission. The graphic shall be in a PANTONE format. The graphic size and location on the SLT shall be large enough to be visually seen from 1 meter, with the unaided eye, prior to encapsulation into the SLS payload shroud.	Complete	
ASD-SLT-029	A mission plan shall be developed to show the SLT design is capable of navigating with the required precision and able to avoid hazards at landing sites. Attitude requirements are to be identified by the team.	Complete	
ASD-SLT-030	Specialized Support Equipment (SE) needed solely for the refitting, refurbishment, repair and refueling of the SLT on the lunar surface shall be included with the delivery of the first flight unit. SLT SE <b>may</b> be delivered to SCS as part of a regular logistics support mission, however, delivery of SE for the first mission must be delivered no later than concurrently with the SLT.	Not started	Expected to satisfy
ASD-SLT-031	The flight SLT and all necessary flight processing hardware shall be delivered to Kennedy Space Center's Multi Payload Processing Facility for launch site processing no later than nine months prior to launch. Initial launch date is currently scheduled for November 2030.	Not started	Expected to satisfy
ASD-SLT-032	The total amount of money that can be provided ("Total Cost Cap") to the project shall be no greater than \$3.9 billion US Dollars (USD) over a 5-year period. Maximum unit cost to build the "launch-ready" SLT shall not exceed: \$0.9 billion USD. The budget report shall show costs comprised of both labor and hardware costs. If the Total Cost Cap is exceeded, then the mission will be canceled.	Not started	Expected to satisfy

## Appendix E: Engineering Change Notices

### Structures

## ENGINEERING CHANGE NOTICE

EAS4700 SPRING 2022

<b>Change Number / Title of change:</b>	STR-001 / Change of truss structure member profiles
<b>Engineering rationale for change:</b>	Previous structure used all hollow cylindrical members, however truss members with hollow square profiles will allow for easier mounting for equipment such as star trackers and panels which have rectangular profiles. This will also allow for less material to be needed for mounting which will lead to less mass for the overall structure.
<b>WAS:</b>	Circular cross-section
<b>IS:</b>	Square cross-section
<b>INITIATOR</b> Name / Email / Function:	Michael Gerber / <a href="mailto:mgerber@ufl.edu">mgerber@ufl.edu</a> / Lead Structures
Team Number / Name:	Team 1/ Lunartics
<b>Collaborator</b> Name / Email/ Function:	N/A
Team Number / Name:	
<b>ADDITIONAL NOTES</b>	This change is only for the main truss structure, the landing gear will still use cylindrical profiles.
<b>- APPROVALS -</b>	
<b>PROJECT MANAGER</b>	
Name / Team Number / email	David Bishop / Lunartics / <a href="mailto:davidbishop@ufl.edu">davidbishop@ufl.edu</a>
Signature / date:	 / April 11, 2022
<b>INSTRUCTOR</b>	
Signature / Email / Date:	<i>Michael Generale</i> / <a href="mailto:mgenerale@ufl.edu">mgenerale@ufl.edu</a> / 11 APR 2022

## Mechanisms

### ENGINEERING CHANGE NOTICE

EAS4700 SPRING 2022

<b>Change Number / Title of change:</b>	#4 / Landing Shock Absorbers
<b>Engineering rationale for change:</b>	Changing the landing dampers to a more reliable design that does not require thermal management and is hermetically sealed to reduce the risk of leaks during repeated landing in the fine lunar dust.
<b>WAS:</b>	Hydraulic damper – Enidine, OEMXT 3/4X1
<b>IS:</b>	Senior Metal Bellows - Metal bellows shock absorber
<b>INITIATOR</b> Name / Email / Function: Team Number / Name:	Jeffrey Glynn / <a href="mailto:michaelglynn@ufl.edu">michaelglynn@ufl.edu</a> / mechanisms and testing Group #1 / Lunartics
<b>Collaborator</b> Name / Email/ Function: Team Number / Name:	N/A
<b>ADDITIONAL NOTES</b>	N/A
<b>- APPROVALS -</b>	
<b>PROJECT MANAGER</b>	
Name / Team Number / email	David Bishop / Group #1 / <a href="mailto:davidbishop@ufl.edu">davidbishop@ufl.edu</a>
Signature / date:	<i>David Bishop</i> 04/04/2022
<b>INSTRUCTOR</b>	
Signature / Email / Date:	<i>Michael Generale</i> <a href="mailto:mgenerale@ufl.edu">mgenerale@ufl.edu</a> / 04APR 2022

## Guidance and Navigation

# ENGINEERING CHANGE NOTICE

EAS4700 SPRING 2022

<b>Change Number / Title of change:</b>	GNC-001/Change of star tracker
<b>Engineering rationale for change:</b>	Need to reduce weight and trade study shows the Sagitta star tracker scores higher in mass, price, and power usage than the HAST star tracker that was previously selected
<b>WAS:</b>	Ball Aerospace HAST
<b>IS:</b>	Arcsec Sagitta Star Tracker
<b>INITIATOR</b> Name / Email / Function:	Kayla Garoust/k.garoust@ufl.edu/Lead GNC
Team Number / Name:	Team 1/Lunartics
<b>Collaborator</b> Name / Email/ Function:	
Team Number / Name:	
<b>ADDITIONAL NOTES</b>	
<b>- APPROVALS -</b>	
<b>PROJECT MANAGER</b>	
Name / Team Number / email	David Bishop/Team 1/davidbishop@ufl.edu
Signature / date:	David Bishop/4/1/2022
<b>INSTRUCTOR</b>	
Signature / Email / Date:	Michael <a href="mailto:mgenerale@mgenerale@ufl.edu">mgenerale@mgenerale@ufl.edu</a> 02 APR 2022

# ENGINEERING CHANGE NOTICE

EAS4700 SPRING 2022

<b>Change Number / Title of change:</b>	GNC-002/Change of IMU
<b>Engineering rationale for change:</b>	Need to reduce weight and trade study shows the M-G370PDS0 outscores the previously selected HG9900 in mass, accelerometer accuracy, and power usage.
<b>WAS:</b>	Honeywell HG9900
<b>IS:</b>	Epson M-G370PDS0
<b>INITIATOR</b> Name / Email / Function:	Kayla Garoust/k.garoust@ufl.edu/Lead GNC
Team Number / Name:	Team 1/Lunartics
<b>Collaborator</b> Name / Email/ Function:	
Team Number / Name:	
<b>ADDITIONAL NOTES</b>	
<b>- APPROVALS -</b>	
<b>PROJECT MANAGER</b>	
Name / Team Number / email	David Bishop/Team 1/davidbishop@ufl.edu
Signature / date:	David Bishop/4/1/2022
<b>INSTRUCTOR</b>	
Signature / Email / Date:	Michael <a href="mailto:mgenerale@mgenerale@ufl.edu">mgenerale@mgenerale@ufl.edu</a> 02 APR 2022

# ENGINEERING CHANGE NOTICE

EAS4700 SPRING 2022

<b>Change Number / Title of change:</b>	GNC-003/Change of Flight Computer
<b>Engineering rationale for change:</b>	Need to reduce weight and trade study shows the Athena-3 flight computer outscores the previously selected Honeywell modified Boeing 787 computers
<b>WAS:</b>	Honeywell Boeing 787 computer
<b>IS:</b>	SEAKR Athena-3
<b>INITIATOR</b> Name / Email / Function:	Kayla Garoust/k.garoust@ufl.edu/Lead GNC
Team Number / Name:	Team 1/Lunartics
<b>Collaborator</b> Name / Email/ Function:	
Team Number / Name:	
<b>ADDITIONAL NOTES</b>	There's not much information available about the Honeywell computers, so keeping this as the design choice provides too many unknowns
<b>- APPROVALS -</b>	
<b>PROJECT MANAGER</b>	
Name / Team Number / email	David Bishop/Team 1/davidbishop@ufl.edu
Signature / date:	David Bishop/4/1/2022
<b>INSTRUCTOR</b>	
Signature / Email / Date:	Michael <a href="mailto:mgenerale@ufl.edu">mgenerale@ufl.edu</a> / 02 APR 2022

## Communications

### ENGINEERING CHANGE NOTICE

EAS4700 SPRING 2022

<b>Change Number / Title of change:</b>	GNC-004/Change of Radio
<b>Engineering rationale for change:</b>	Trade study results show the BCT SDR is superior to the SDL IRIS in regards to mass, data rate, and power usage
<b>WAS:</b>	Space Dynamics Laboratory IRIS
<b>IS:</b>	Blue Canyon Technologies SDR
<b>INITIATOR</b> Name / Email / Function:	Kayla Garoust/k.garoust@ufl.edu/Lead GNC
Team Number / Name:	Team 1/Lunartics
<b>Collaborator</b> Name / Email/ Function:	
Team Number / Name:	
<b>ADDITIONAL NOTES</b>	
<b>- APPROVALS -</b>	
<b>PROJECT MANAGER</b>	
Name / Team Number / email	David Bishop/Team 1/davidbishop@ufl.edu
Signature / date:	David Bishop/4/1/2022
<b>INSTRUCTOR</b>	
Signature / Email / Date:	Michael <a href="mailto:mgenerale@mgenerale@ufl.edu">mgenerale@mgenerale@ufl.edu</a> 02 APR 2022

### ENGINEERING CHANGE NOTICE

EAS4700 SPRING 2022

<b>Change Number / Title of change:</b>	GNC-005/X-band Amplifier
<b>Engineering rationale for change:</b>	Trade study results show the TGM2635-CP outscores the previously selected X-band SSPA in mass, output power, frequency range, and input power.
<b>WAS:</b>	General Dynamics X-band SSPA
<b>IS:</b>	Qorvo TGM2635-CP
<b>INITIATOR</b> Name / Email / Function:	Kayla Garoust/k.garoust@ufl.edu/Lead GNC
Team Number / Name:	Team 1/Lunartics
<b>Collaborator</b> Name / Email/ Function:	
Team Number / Name:	
<b>ADDITIONAL NOTES</b>	
<b>- APPROVALS -</b>	
<b>PROJECT MANAGER</b>	
Name / Team Number / email	David Bishop/Team 1/davidbishop@ufl.edu
Signature / date:	David Bishop/4/6/2022
<b>INSTRUCTOR</b>	
Signature / Email / Date:	

## ENGINEERING CHANGE NOTICE

EAS4700 SPRING 2022

<b>Change Number / Title of change:</b>	GNC-006/S-band Amplifier
<b>Engineering rationale for change:</b>	Trade study results show the PE15A5003 outscores the previously selected S-band SSPA in mass, output power, and frequency range.
<b>WAS:</b>	General Dynamics S-band SSPA
<b>IS:</b>	Pasternack PE15A5003
<b>INITIATOR</b> Name / Email / Function:	Kayla Garoust/k.garoust@ufl.edu/Lead GNC
Team Number / Name:	Team 1/Lunartics
<b>Collaborator</b> Name / Email/ Function:	
Team Number / Name:	
<b>ADDITIONAL NOTES</b>	
<b>- APPROVALS -</b>	
<b>PROJECT MANAGER</b>	
Name / Team Number / email	David Bishop/Team 1/davidbishop@ufl.edu
Signature / date:	David Bishop/4/6/2022
<b>INSTRUCTOR</b>	
Signature / Email / Date:	

## ENGINEERING CHANGE NOTICE

EAS4700 SPRING 2022

<b>Change Number / Title of change:</b>	GNC-007/Removal of Transponder
<b>Engineering rationale for change:</b>	Research of satellite communications shows no need for a separate transponder other than for redundancy purposes. An additional SDR will be used instead to fulfill the need for redundancy since the selected SDR performs the same functions and more than the previously selected transponder.
<b>WAS:</b>	General Dynamics S-band SSPA
<b>IS:</b>	Adding additional SDR
<b>INITIATOR</b> Name / Email / Function:	Kayla Garoust/k.garoust@ufl.edu/Lead GNC
Team Number / Name:	Team 1/Lunartics
<b>Collaborator</b> Name / Email/ Function:	
Team Number / Name:	
<b>ADDITIONAL NOTES</b>	
<b>- APPROVALS -</b>	
<b>PROJECT MANAGER</b>	
Name / Team Number / email	David Bishop/Team 1/davidbishop@ufl.edu
Signature / date:	David Bishop/4/6/2022
<b>INSTRUCTOR</b>	
Signature / Email / Date:	

## Appendix F: SLT Size Verification

SLT dimensions:

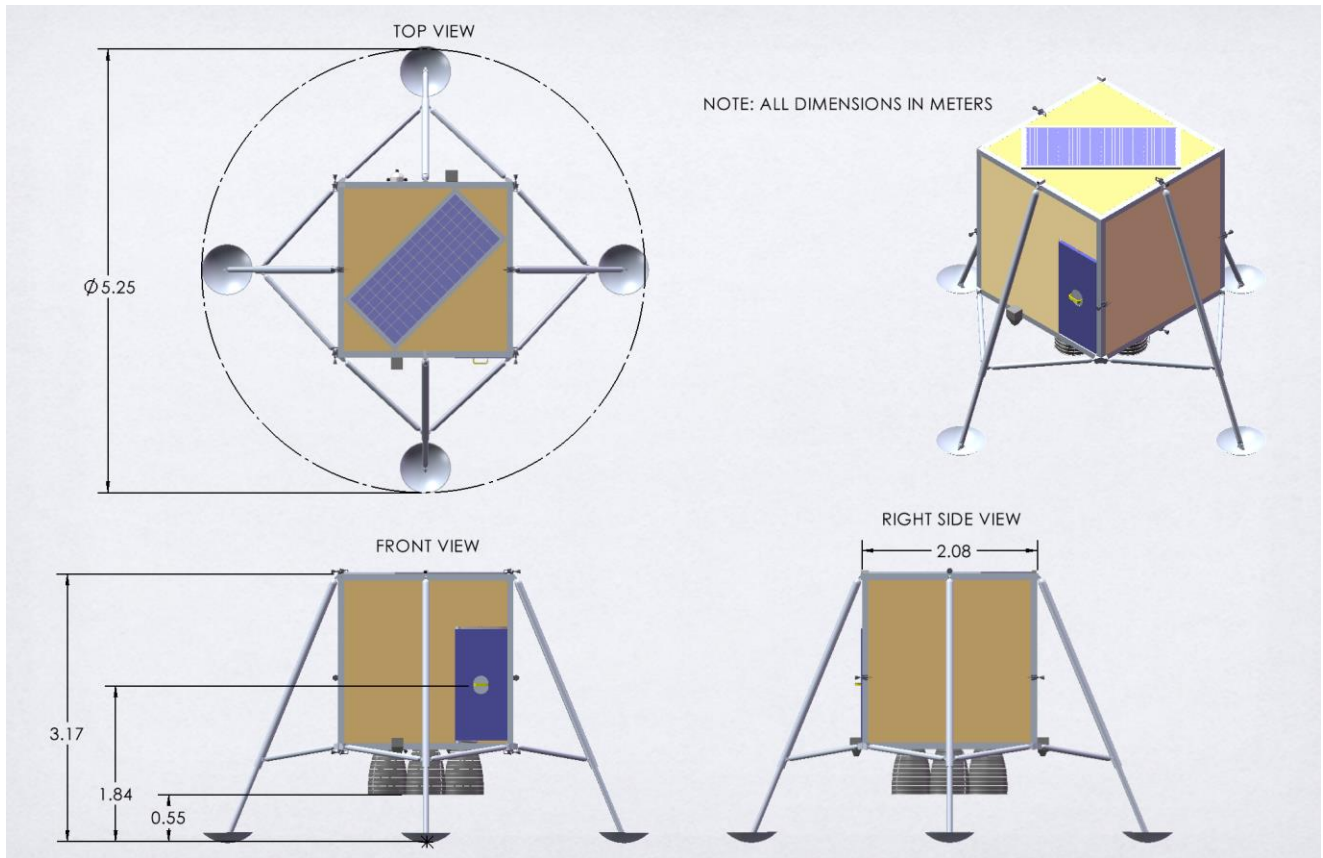
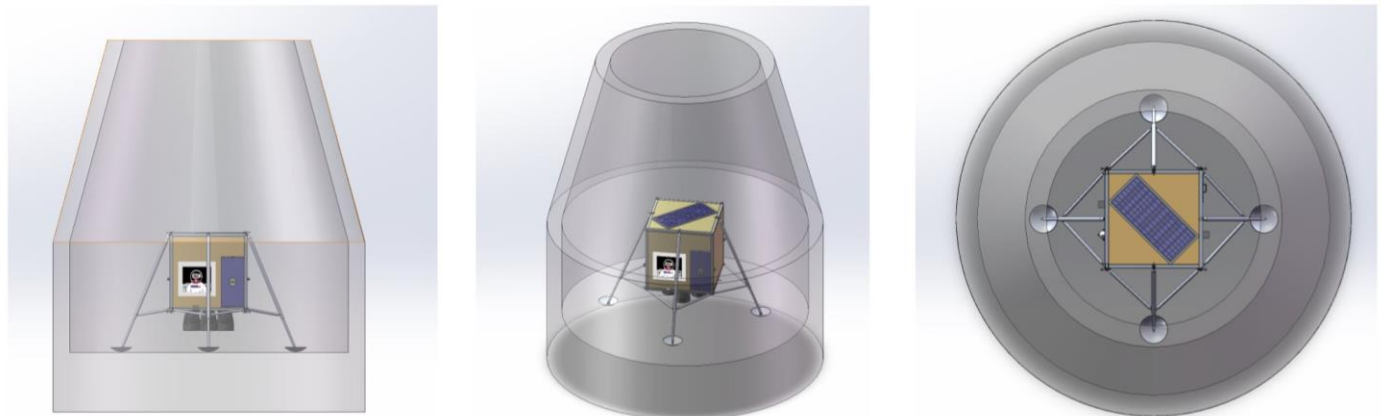


Figure 82. Size of the SLT (dimensions in meters).

SLS size verification:



**Note: 1.02 m of clearance between outer footpad circle and the SLS module inner wall**

*Figure 83. Verification of the SLT in the 8.4m diameter SLS capsule. Shown from left to right, are the side view, isometric view, and top view.*

## Appendix G: Center of Mass and Mass Properties

Center of Mass (without payload):

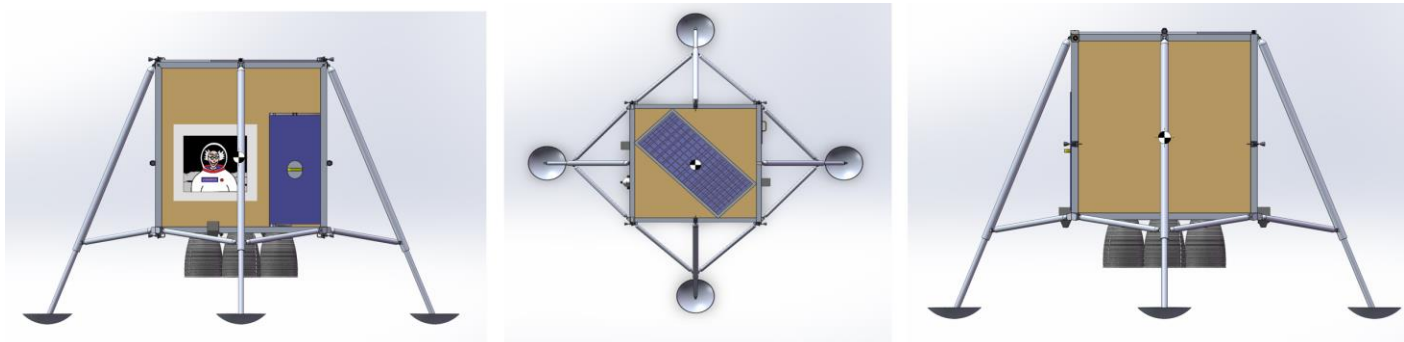


Figure 84. Center of Mass of SLT with payload removed.

Center of Mass (with payload):

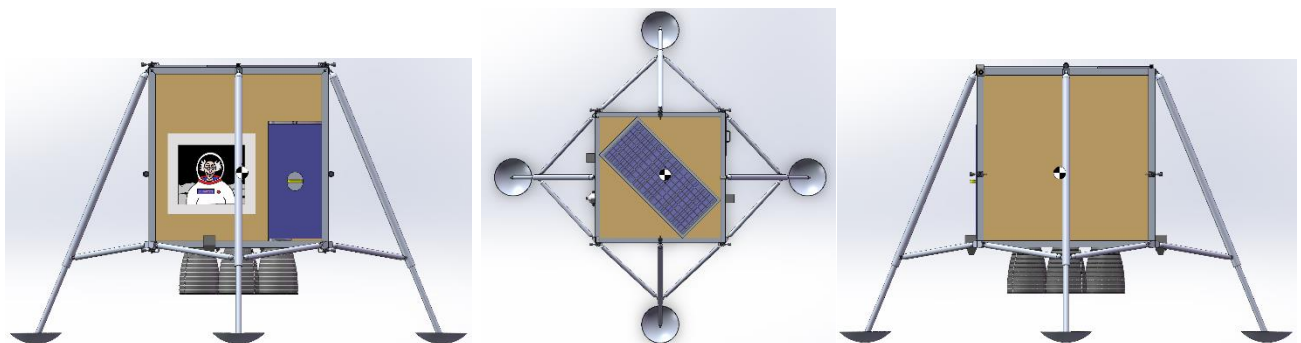


Figure 85. Center of Mass of SLT with payload attached.

## **Mass Properties:**

- Wet Mass (including payload) = 2188.021 kg
- Wet Mass (excluding payload) = 1988.021 kg
- Dry Mass (including payload) = 850.851 kg
- Dry Mass (excluding payload) = 650.851 kg

The following information is taken for the SLT without the payload included.

- Center of Mass: (meters)
  - X = 0.56
  - Y = 0.94
  - Z = 1.75
- Principal axes of inertia and principal moments of inertia: (kg \* square meters)  
Note: Taken from center of mass.
  - I<sub>x</sub> = (-0.47, -0.18, 0.86)      P<sub>x</sub> = 1610.06
  - I<sub>y</sub> = (0.88, -0.21, 0.43)      P<sub>y</sub> = 1725.16
  - I<sub>z</sub> = (0.10, 0.96, 0.26)      P<sub>z</sub> = 1778.56
- Moments of inertia: (kilograms \* square meters)  
Note: Taken at the center of mass and aligned with the output coordinate system.
  - L<sub>xx</sub> = 1700.22 L<sub>xy</sub> = 4.52      L<sub>xz</sub> = -48.18
  - L<sub>yx</sub> = 4.52      L<sub>yy</sub> = 1770.82 L<sub>yz</sub> = -30.97
  - L<sub>zx</sub> = -48.18      L<sub>zy</sub> = -30.97      L<sub>zz</sub> = 1642.74
- Moments of inertia: (kilograms \* square meters)  
Note: Taken at the output coordinate system.
  - I<sub>xx</sub> = 6953.51 I<sub>xy</sub> = 711.34      I<sub>xz</sub> = 1262.08
  - I<sub>yx</sub> = 711.34      I<sub>yy</sub> = 6261.85 I<sub>yz</sub> = 2164.13
  - I<sub>zx</sub> = 1262.08      I<sub>zy</sub> = 2164.13 I<sub>zz</sub> = 3248.79